Geol. Mag. **153** (*2*), *2016, pp. 332–354.* © *Cambridge University Press 2015*
doi:10.1017/S0016756815000643

A tale of two extinctions: converging end-Permian and end-Triassic scenarios

BAS VAN DE SCHOOTBRUGGE*† & PAUL B. WIGNALL‡

*Marine Palynology & Paleoceanography, Institute of Earth Sciences, Utrecht University, Utrecht, Heidelberglaan 2, 3584 CS, The Netherlands
‡School of Earth and Environment, University of Leeds, Leeds LS2 9JT, UK

(*Received* 19 December 2014; *accepted* 5 August 2015; *first published online* 26 October 2015)

Abstract – The end-Permian (*c.* 252 Ma) and end-Triassic (*c.* 201 Ma) mass-extinction events are commonly linked to the emplacement of the large igneous provinces of the Siberia Traps and Central Atlantic Magmatic Province, respectively. Accordingly, scenarios for both extinctions are increasingly convergent and cross-fertilization of ideas has become important. Here, we present a synthesis of extinction scenarios based on a critical assessment of the available palaeontological, sedimentological, geochemical and geophysical evidence. How similar were the extinction events, what gaps exist in our understanding and how can a comparison of the events enhance our understanding of each event individually? Our focus is on the most important proximate kill mechanisms including: climate change and atmospheric pollution; increased soil erosion, weathering and runoff; forest dieback and the spread of pathogens; and ocean temperature changes, anoxia and acidification. There is substantial evidence to suggest that very similar kill mechanisms acted upon late Permian as well as Late Triassic ecosystems, strengthening the hypothesis that the ultimate causes of the mass-extinction events were similar.

Keywords: mass extinction, Permian, Triassic, Jurassic, proximate kill mechanisms.

1. Introduction

The Triassic Period (252–201 Ma) remains an intriguing time interval that witnessed both unbridled eruptions of life, exemplified by the towering coral reefs that are preserved in the Northern Calcareous Alps of Austria, as well as utter devastation during two of the largest mass-extinction events of the past 600 million years that wiped out ecosystems on a global scale. Of these two extinction events the end-Permian mass-extinction (EPME) is the largest, terminating many Palaeozoic lineages of life at the same time as heralding the advent of Mesozoic organisms and laying the foundations for the so-called Modern Fauna (Sepkoski Jr, 1987, 1996; Erwin, 1993). The end-Triassic mass-extinction (ETME), albeit smaller in numbers of extinct genera (Bambach, 2006), led to equally dramatic changes in ecosystem composition and structure and altered sedimentation style in basins around the world for millions of years (Hallam, 1993; van de Schootbrugge *et al.* 2013).

It is impossible to briefly summarize the many intricacies of the changes in biodiversity associated with both extinction events; however, broad trends can be described. Both extinction events led to near-annihilation of cnidarian clades and other taxa responsible for reef construction, resulting in 'reef gaps' that lasted millions of years (Stanley, 1988, 2003; Stanley & Beauvais, 1994). Other clades of marine invertebrates, such as molluscs including ammonoids, gastropods and bivalves, were hard hit in both instances (Kiessling *et al.* 2007). Following the end-Triassic extinction, Early Jurassic shallow seas witnessed recurrent euxinia over a time span of 25 million years, culminating in the Toarcian Oceanic Anoxic Event (Richoz *et al.* 2012; van de Schootbrugge *et al.* 2013). Widespread euxinia also characterized shallow-marine settings bordering the Tethys Ocean in the direct aftermath of the end-Permian extinction (Wignall & Hallam, 1992; Grice *et al.* 2005*a*). Black shales deposited across both extinction events are characterized by an abundance of fossilized pigments that derive from green sulphur bacteria, indicating that euxinic conditions developed close to the surface of the oceans (Grice *et al.* 2005*a*; Richoz *et al.* 2012). On land, forest dieback during both events was accompanied by the proliferation of opportunists and pioneers, including ferns and fern allies (Looy *et al.* 2001; van de Schootbrugge *et al.* 2009). Furthermore, both events led to major schisms in the dominant terrestrial herbivores (Benton, 1986; Benton, Tverdokhlebov & Surkov, 2004) and apex predators, including the late Permian extinction of the pariaeosaurs and many dicynodonts and the end-Triassic loss of crurotarsans (Olsen *et al.* 2002).

A considerable number of reviews and books on either the end-Permian or the end-Triassic have been written over the past 20 years (Erwin, 1993; Knoll *et al.* 1996; Hallam & Wignall, 1997; Benton & Twitchett, 2003; Tanner, Lucas & Chapman, 2004; Hesselbo, McRoberts & Palfy, 2007; Algeo *et al.* 2011; Payne & Clapham, 2012; Benton & Newell, 2014; Wignall, 2015), summarizing a rapidly growing body of work

†Author for correspondence: B.vanderSchootbrugge@uu.nl

on either extinction event. Here, we synthesize and compare the recent work on both the end-Permian and end-Triassic extinction events. Starting with the main premise that both extinction events were triggered by the emplacement of large igneous provinces, we focus on a comparison of kill mechanisms resulting from flood basalt volcanism. The purpose of such a review is to detect similarities and/or pronounced differences that can promote an understanding of either event. Moreover, gaps in our understanding of specific aspects, or lack of data, can be brought to light.

Large-scale volcanism or extraterrestrial impacts are widely considered to have been the two main extinction triggers of mass extinctions that set in motion a chain of adverse environmental and biotic changes, the so-called proximate kill mechanisms. An extinction trigger for the EPME that has been discussed by a relatively small number of authors is the role of extraterrestrial impacts, in analogy to scenarios for the Cretaceous–Palaeogene extinction. However, there is currently no conclusive evidence for bolide impact at or near the end-Permian extinction horizon. Claims for the presence of extra-terrestrial fullerenes at the Permian–Triassic boundary (Becker *et al.* 2001), chondritic fragments present in a section in Antarctica (Basu *et al.* 2003) and a supposed impact crater at Bedout (Western Australia; Becker *et al.* 2004) have neither been replicated, accepted nor confirmed in any other work. The most important argument against an extra-terrestrial impact comes from the fossil record. The stepped nature of the end-Permian extinction with losses beginning in the latest Permian and continuing into the Triassic (Algeo *et al.* 2011; Song *et al.* 2013) would require multiple giant impacts. Recent calibration of the end-Permian extinction indicates it climaxed around 252.3 Ma, spanning at least several hundreds of thousands of years (Shen *et al.* 2011*a*). Statistical treatment of last occurrences from a number of sections across China also suggest that conditions started to deteriorate 1.2 million years before the extinction horizon (Wang *et al.* 2014). Such findings are difficult to reconcile with a single catastrophic event.

Debates on the relationship between Late Triassic impacts and the end-Triassic extinction have continued to flare up. A number of impact craters have ages close to the Triassic–Jurassic boundary, but none have a size that is large enough to be considered as an impactor driving extinction (Fig. 1). The hypothesis of 'multiple Late Triassic impacts' centred on 214 Ma (Spray, Kelley & Rowley, 1998) can be confidently put to rest based on improved dating of several of the craters (Schmieder *et al.* 2014), which conclusively shows that the impacts occurred over an interval of more than 50 million years rather than hours as suggested by Spray, Kelley & Rowley (1998). The Obolon crater in Ukraine was recently re-dated by Gurov *et al.* (2009) to have a Bajocian age (169 ± 7 Ma), whereas the Lake Saint Martin crater was dated to be of Carnian age (227 ± 0.9 Ma) by Schmieder *et al.* (2014). The most close in age, the Rochechouart crater in France with a diameter of *c.* 25 km, was recently re-dated to 202.8 ± 2 Ma (Schmieder *et al.* 2010), overlapping with the end-Triassic extinction. Its size is modest and of the same order as other impacts however, such as the Miocene Nördlinger Ries-Steinheim binary impact in southern Germany that had no noticeable effect on global biodiversity (Böhme, Gregor & Heissig, 2002).

Evidence that could link Rochechouart or other (undiscovered) craters with the end-Triassic extinction has been scarce. Findings of shocked quartz in a number of shale beds in Italy (Bice *et al.* 1992) have not been confirmed or replicated in other sections. A modest iridium anomaly (in the range of parts per trillion) in the Newark Basin that co-occurs with abundant fern spores has been attributed to an impact (Olsen *et al.* 2002); however, it is increasingly doubtful whether this level really represents the end-Triassic extinction event (Wotzlaw *et al.* 2014), or if it corresponds to a precursor event (Cirilli *et al.* 2009). In fact, no 'smoking gun' has been found to implicate a large bolide impact as the cause of the end-Triassic extinction. Small iridium spikes in the Upper Triassic Blomidon Formation in Nova Scotia (Canada) in proximity to a large basalt flow are likely products of volcanic eruptions (Tanner, Kyte & Walker, 2008), whereas in Austria clay spherules at the top of the regionally significant Rhaetian Kössen Formation have also been interpreted to originate from volcanic fall-out (Zajzon *et al.* 2012). Neither of these studies reported on co-occurring shocked-quartz minerals or any other bona fide extra-terrestrial impact indicators. Despite intensive searches other authors have failed to detect iridium, for example in marginal-marine to continental strata in Poland (Pienkowski, Niedzwiedzki & Waksmundzka, 2012) as well as shallow-marine strata in Denmark (Sofie Lindström, pers. comm. 2014).

Finally, widespread soft sediment deformations in sections across the UK were initially attributed to a single impact event, presumably in the Irish Sea (Simms, 2003). However, where sections are more complete the seismites are separated by undisturbed beds, suggesting a number of large earthquakes (Lindström *et al.* 2015). There is in fact evidence for synsedimentary tectonic activity from the same sections (Wignall & Bond, 2008), for example at Pinhay Bay where the upper Rhaetian deposits contain a thick debrite bed, and evidence for polygonal faults that have deformed the lowermost Jurassic Blue Lias sediments (Fig. 2).

The evidence for widespread seismites in the Rhaetian of NW Europe could be linked to the emplacement of a large igneous province. Instead of extra-terrestrial bolide impacts, both the end-Permian and end-Triassic extinction events appear to be Earth-bound disasters. These are both coeval with the emplacement of two of the largest flood basalt provinces of Phanerozoic time, seen by most workers as the principal trigger for environmental changes leading to mass extinction (Courtillot, 1994; Wignall, 2001*a*; Palfy, 2003;

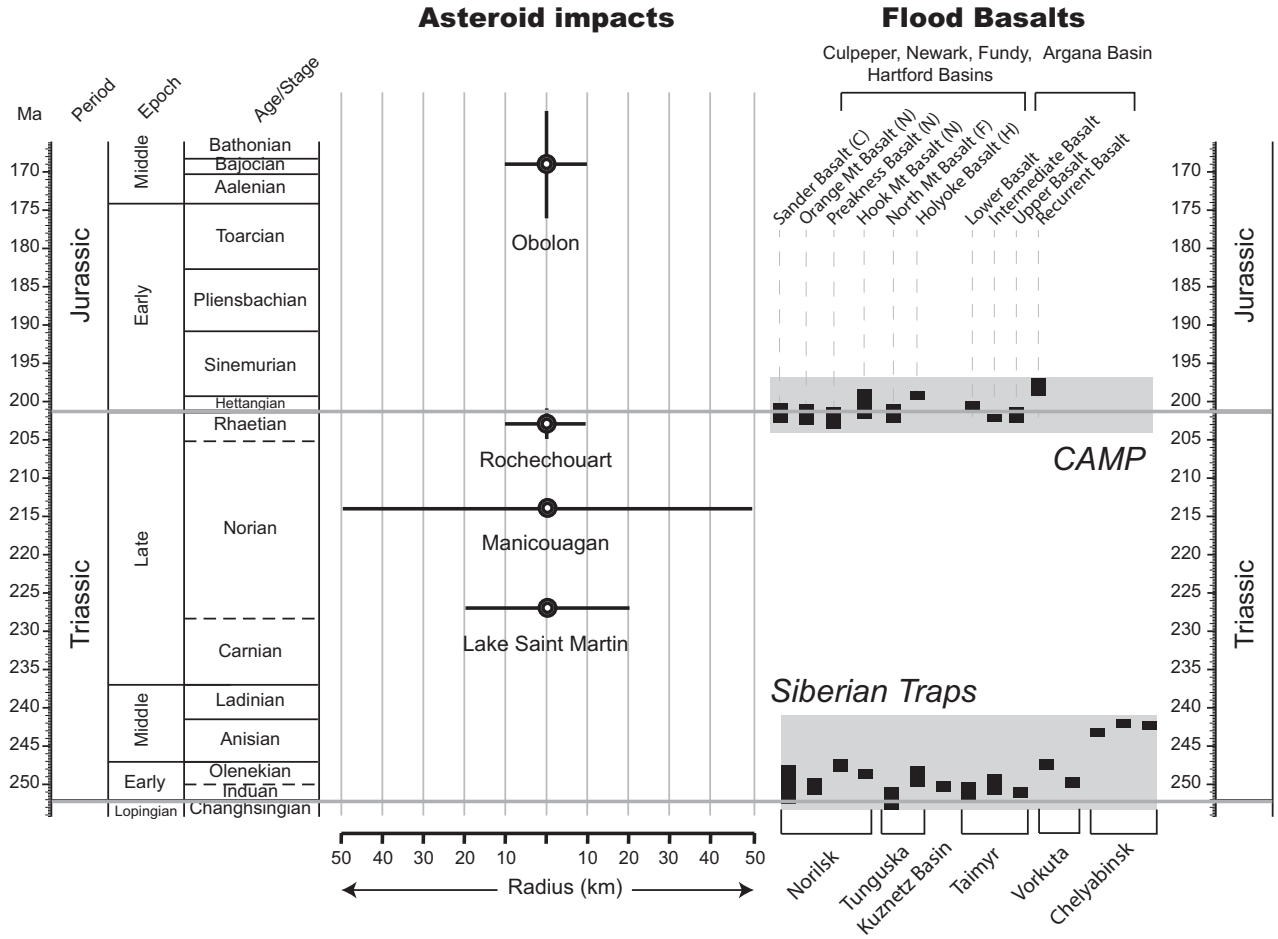

Figure 1. Overview of radiometric dated occurrences of impact craters (modified after Schmieder *et al.* 2014) and flood basalt flows, sills and dykes (Siberian Traps: Reichow *et al.* 2009; CAMP: Marzoli *et al.* 2011; Blackburn *et al.* 2013). The age for the Norian–Rhaetian boundary (205.3 Ma) is modified after Wotzlaw *et al.* (2014). The timescale was created with the free shareware TimescaleCreator v6.3.

Svensen *et al.* 2009; Payne & Clapham, 2012; Bond & Wignall, 2014). Radiometric dating of zircons obtained from ash beds close to the biostratigraphically defined Permian–Triassic boundary in the global stratotype section and point (GSSP) of Meishan in China (Bowring *et al.* 1998; Burgess, Bowring & Shen, 2014) and from basalt flows in the Siberian Traps large igneous province (LIP) are virtually indistinguishable (Reichow *et al.* 2009). Volcanism was intense during earliest Triassic time, but there are radiometric dates of younger phases in locations such as Chelyabinsk (Fig. 1).

The emplacement of the Central Atlantic Magmatic Province figures prominently in scenarios for the end-Triassic extinction (Palfy, 2003; Nomade *et al.* 2006; Hesselbo, McRoberts & Palfy, 2007). Despite this general consensus, the exact timing of flood basalt eruptions and its impact on ecosystems remain to be firmly established. Central Atlantic Magmatic Province (CAMP) extrusives have been thought to straddle the Triassic–Jurassic boundary (Marzoli *et al.* 1999, 2004) and the eruptions estimated to have taken place over an interval of not less than 600 ka but not more than 1 Ma (Knight *et al.* 2004; Nomade *et al.* 2006). Improved dating of the actual Triassic–Jurassic boundary in sections in Peru that contain ash beds calibrated with ammonite stratigraphy place the boundary at 201.36 ± 0.17 Ma (Schaltegger *et al.* 2008; Schoene *et al.* 2010). This age is indistinguishable from the age of the North Mountain Basalt, the oldest basalt flow in the Fundy Basin (Marzoli *et al.* 2011). At least four major pulses of sill and dyke emplacement as well as fissure eruptions have been dated to occur directly following the biostratigraphically defined Triassic–Jurassic boundary in the NE United States (Blackburn *et al.* 2013) and Morocco (Knight *et al.* 2004).

While the correspondence between the onset of CAMP volcanism and the Triassic–Jurassic boundary is certain, it is important to note that most extinction losses pre-date the period boundary. However, there is indirect evidence for volcanism prior to the onset of flood basalts in Morocco where mudstones derived from weathering of mafic volcanic rocks underlie the first lava flows (Dal Corso *et al.* 2014). It is possible that volcanism may have occurred even earlier in undated and little explored parts of the volcanic province, such as in the Amazon Basin. Proxy evidence for eruptions starting during the early Rhaetian Stage is provided by a decline in the $^{187}Os/^{188}Os$ at this time (Kuroda *et al.* 2010).

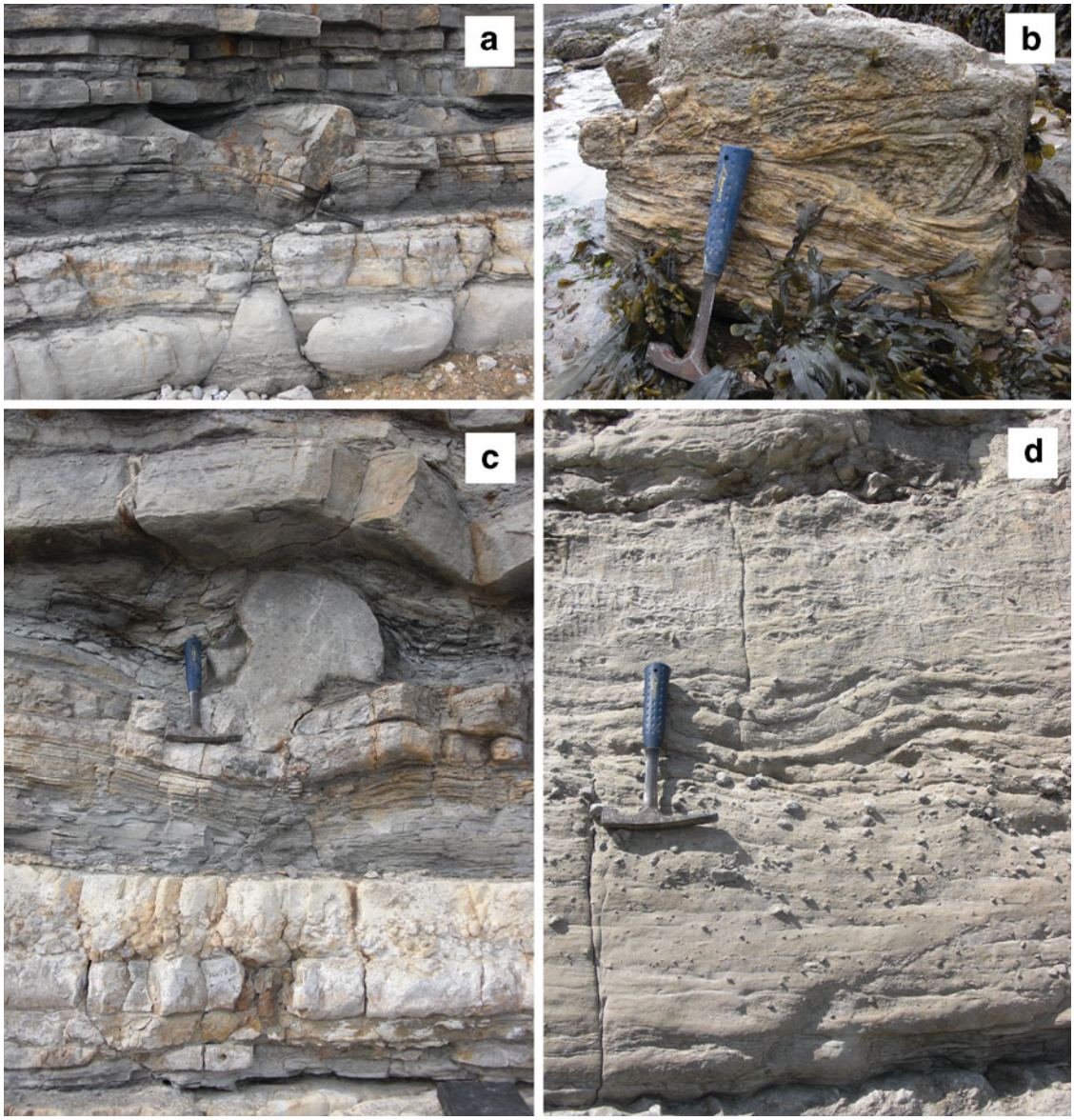

Figure 2. (Colour online) (a) Synsedimentary tectonics within the base of the Blue Lias Formation at Pinhay Bay (close to Lyme Regis). Compare figure 3 of Wignall (2001*b*). Small polygonal fault sets leading to soft-sediment deformation. (b) Slump folds within the Cotham Member of the Lilstock Formation on the foreshore of St Audrie's Bay. (c) Soft sediment deformation within the base of the Blue Lias Formation at Pinhay Bay (close to Lyme Regis). Compare figure 3 of Wignall (2001*b*). (d) Calcareous debris-flow bed within the upper part of the Cotham Member. Compare figure 3 of Wignall (2001*b*).

2. The atmosphere

2.a. Atmospheric pollution

The most immediate effect of volatile release from flood basalt volcanism would have been changes in atmospheric chemistry, with regional to global deleterious effects on terrestrial ecosystems and organisms from plants to herbivores. The example of the Laki Fissure eruption of 1783–84 is a powerful reminder of the way in which even small events can have serious consequences. Following the Laki eruption, the severe loss of livestock on Iceland was attributed to the release of large amounts of fluorine and chlorine (Grattan, 2005). Even larger amounts of sulphur dioxide reached continental Europe as a sulphuric haze, leading to failed crops and unusual summer weather (Chenet, Fluteau & Courtillot, 2005). The eruption lasted for several months and produced about 12 km^3 of basalt, which is several orders of magnitude smaller than the individual eruptions that formed the Siberian Traps and CAMP large igneous provinces. Based on melt inclusions from Siberian Traps flood basalts, Black *et al.* (2013) presented a compelling case for previously underestimated volatile loads. Not only did the Siberian Traps release large amounts of sulphur (*c.* 6300–7800 Gt S), but vast amounts of chlorine (*c.* 3400–8700 Gt Cl) and fluorine (*c.* 7100–13 600 Gt F) were also released.

Even though activity within the Siberian Traps and CAMP was spread out over several hundreds of thousands of years, climactic phases are thought to have been brief, coincident with the rapid emplacement of large volumes of basalt both as sills and dykes and

large surface flows (Knight *et al.* 2004). Precise estimates of fluorine and chlorine are not available for CAMP basalts, but SO_2 release was recently evaluated by Callegaro *et al.* (2014) based on melt inclusions. Results from that study show that CAMP flood basalts could have released up to 8 Mt of SO_2 per km^3 of erupted basalts or up to 8000 Gt for the entire province, placing CAMP emissions within the same range as the Siberian Traps.

Sulphur dioxide released to the atmosphere quickly combines with hydroxyl (OH^-) and oxygen to form sulphur trioxide which, after reaction with water, leads to sulphuric acid droplets. These have a cooling effect in the troposphere, and rain out as acid rain after only weeks to months. The effect of SO_2 release on the atmosphere and subsequent cooling events were therefore short-lived. In contrast, the impact of sulphur deposition on soils and vegetation was likely more severe. Sulphur deposition in the form of acid rain has been invoked for the end-Permian extinction based on high sulphide concentrations in lacustrine sediments in the Karoo Basin (South Africa; Maruoka *et al.* 2003) and from the presence of soil-pH-sensitive vanillin molecules in Italian boundary shales (Sephton *et al.* 2015). Evidence for acid rain related to CAMP eruptions is unfortunately even more circumstantial. A peculiar darkening of pollen and spores recovered from Triassic–Jurassic boundary sediments in Germany, Denmark and Poland has been tentatively attributed to soil acidification (van de Schootbrugge *et al.* 2009; Pienkowski, Niedzwiedzki & Branski, 2014).

The effects of widespread acid rain on fresh water and forest ecosystems as well as individual plant species have been studied in great detail during the last decades of the twentieth century, when large tracts of North American and European forests started to suffer from industrial emissions of sulphur dioxide from coal-fired power plants (Bricker & Rice, 1993). Acid rain triggered a complex suite of changes during the 1970s and 80s that led to widespread forest dieback, especially in the so-called 'Black Triangle' at the borders of Germany, Czech Republic and Poland (Ulrich, 1990). Intense research concluded that the most important result of acid rain was to alter soil conditions leading to the leaching of the essential cations Ca, K and Mg, which would then be quickly lost during rainfall events (Tomlinson, 2003). In addition, severe damage to root systems, due to lowered soil pH, constituted a further weakening of the affected pine forests (Tomlinson, 2003). Discolouration and loss of leaves/needles was also observed and attributed to direct impact of acid rain on the canopy (Evans, 1984).

Volcanic sulphuric hazes and acid rain likely constituted proximate kill mechanisms for plants during both the end-Permian and end-Triassic extinction events. The effects of direct fumigation of plants with SO_2 has been studied both in the field, for example in Hawaii (Tanner, Smith & Allan, 2007; Winner & Mooney, 1980*a*, *b*), as well as in mesocosm experiments (Elliott-Kingston, Haworth & McElwain, 2014). Pines growing in the vicinity of sulphur degassing fumaroles at Campi Flegrei (southern Italy) showed significant damage to epicuticular waxes (Bartiromo *et al.* 2012), while fumigation of ten species of plants representative of Mesozoic conifer and fern vegetation showed consistent damage to epicuticular waxes in all specimens (Elliott-Kingston, Haworth & McElwain, 2014). Other effects included the appearance of lesions on the stomata and distortions to the stomatal complex. Mesocosm experiments in China, a country currently heavily affected by SO_2 pollution from domestic and industrial coal burning, showed that the air concentration of SO_2 is more important in damaging crops than the duration of fumigation (Cao, 1989). In controlled experiments, plant damage included a reduction in chlorophyll, inhibition of photosynthesis and a damage to plant tissues related to the presence of free oxygen radicals (Cao, 1989). Translated to the end-Permian or end-Triassic, this would mean that brief pulses of intense flood basalt activity with high levels of sulphur dioxide emissions would be more devastating than slow long-term degassing of basalts.

In addition to gaseous volatiles, other pollutants may have had a dramatic impact on both the atmosphere and biosphere beneath it. It remains unclear whether, in the early stages of LIP emplacement, fire fountains could have been violent enough to directly inject volatiles into the stratosphere where their effect would be global rather than regional (Self *et al.* 2006). If so, bromine and chorine complexation with organic molecules (organohalogens) may have damaged the ozone layer, potentially leading to dangerously high levels of UV-radiation (Visscher *et al.* 2004). Model runs by Beerling *et al.* (2007) indicate that collapse of the ozone layer would have been possible, assuming large amounts of chlorinated organics (e.g. $ClCH_3$) were generated via intrusion of Siberian Traps magma into evaporites and organic-rich strata (Black *et al.* 2013).

Mutagenesis observed in the Lower Triassic herbaceous lycopsid *Isoetales* has been attributed to increased levels of UV-radiation under low ozone conditions (Visscher *et al.* 2004). The widespread occurrence of unseparated *Isoetales*-tetrads of the form genera *Kraeuselisporites*, *Lundbladispora* and *Uvaesporites* has been linked to genetic mutation either inhibiting successful reproduction or signalling the ability of lycopsids to adapt to drought-prone habitats and reproduce asexually (Visscher *et al.* 2004). Mutations also appear evident in pollen. Aberrant pollen, such as trisaccate forms of normally bisaccate pollen, have been described from several sections straddling the Permian–Triassic boundary in Russia and China (Foster & Afonin, 2005; Metcalfe *et al.* 2009).

Visscher *et al.* (2004) alluded to the fact that the end-Triassic extinction was equally associated with abundant unseparated tetrads belonging to *Kraeuselisporites reissingerii,* again derived from a lycopsid parent plant. A distinct early Hettangian spike in tetrads was noted and quantified in sections from Austria (Bonis, Kürschner & Krystyn, 2009), Germany (van

de Schootbrugge *et al.* 2009; Heunisch *et al.* 2010) and Denmark and Sweden (Lindström *et al.* 2012). Mutagenesis of *Classopollis*-pollen (Kürschner, Batenburg & Mander, 2013), particularly the occurrence of malformed tetrads, has also been discussed as evidence for environmental stress. Previously unpublished data by one of the authors (BvdS) from cores in Germany and Luxemburg indicates the presence of teratological tetrads and aberrant pollen in lowest Hettangian deposits (Fig. 3), but further work is needed to quantify the occurrences. *Ricciisporites tuberculatus*, an enigmatic gymnosperm unseparated pollen-tetrad, likely represents another possible pollen taxon that shows aberrant morphology in the form of its bizarre and highly variable wart-like wall structure. *Ricciisporites* (and its pollen-producing parent plant) became one of the most prominent victims of the end-Triassic extinction event across NW Europe (van de Schootbrugge *et al.* 2009; personal observations).

Sulphur dioxide was perhaps the most abundant toxin released but smaller quantities of other more toxic pollutants, such as heavy metals and polycyclic aromatic hydrocarbons (PAHs), likely had a deleterious impact on terrestrial ecosystems. High concentrations of mercury (Hg) have been detected in Permian–Triassic sections in the Sverdrup Basin (Canada; Grasby, Sanei & Beauchamp, 2011). The only plausible source of these highly toxic metals were the Siberian Traps. Mercury may have adsorbed onto coal fly-ash particles generated during subsurface thermal metamorphism of coal beds (Grasby, Sanei & Beauchamp, 2011; Grasby *et al.* 2015). It is increasingly clear that the lethal effects of large igneous provinces are strongly enhanced when lava metamorphoses crustal rocks during ascension, particularly during sill emplacement (Ganino & Arndt 2009). The potential to generate additional large quantities of greenhouse gases CO_2 and CH_4, and pollutants including SO_2, largely depends on the subsurface presence of sediments rich in coal, organic matter, petroleum or evaporites. In the Tunguska Basin in Siberia, large kilometre-wide volcanic breccia pipes occur throughout the Siberian Traps province; the effects of the Siberian Traps volcanism may have been greatly exacerbated by lava intrusions into Palaeozoic hydrocarbon reservoirs (Svensen *et al.* 2009).

For the CAMP, the relationship between thermogenesis and volcanism is harder to demonstrate. Intrusion into Permian evaporites in the Amazon Basin is suspected but has not been conclusively demonstrated (Svensen *et al.* 2009). In the Deep River and Sanford basins in North Carolina (United States) dykes and sills belonging to the CAMP are in contact with Carnian coals, where a substantial volume of coal has been transformed into natural cokes (Reinemund, 1955). Van de Schootbrugge *et al.* (2009) attributed elevated concentrations in polycyclic aromatic hydrocarbons (PAHs) in Triassic–Jurassic core samples from north Germany to the subsurface thermal metamorphism of coals and organic-rich sediments. This interpretation was based on the notion that mainly high-molecular-weight (HMW) PAH, such as coronene, were dominating PAH contents of latest Triassic samples. These 5- and 6-ring PAHs form due to high-temperature charring of organic matter and coal (Fig. 4). It is unlikely that these PAH in the late Rhaetian Triletes Beds were sourced from sills in North Carolina. It is not only the large distance which may be a factor in this theory, but the latest radiometric dating shows these sills to have ages of *c.* 200 Ma, that is, almost 1.5 Ma after the Triassic–Jurassic boundary (Blackburn *et al.* 2013).

2.b. Climate change

The residence time of carbon dioxide in the atmosphere is considerably longer than sulphur dioxide and other pollutants, and its residence time in the global carbon cycle is of the order several hundreds of thousands of years (e.g. Katz *et al.* 2005). Dramatic and rapid excursions in carbon isotope records reflecting major carbon cycle perturbations have been documented based on a variety of archives, including bulk carbonate (Payne *et al.* 2004; Bachan *et al.* 2012; Shen *et al.* 2013), macro- and microfossil skeletal carbonate (Joachimski *et al.* 2012), bulk organic matter (Hesselbo *et al.* 2002) and organic molecules (Whiteside *et al.* 2010; Ruhl *et al.* 2011). At face value all these records, in addition to numerous others, indicate one or multiple large negative C-isotope excursions (CIE) for both the Permian–Triassic and Triassic–Jurassic boundaries. However, strong differences exist between the expression and recording of the carbon cycle perturbations in marine and terrestrial settings. The main negative CIE at the Triassic–Jurassic boundary appears strongly amplified in cuticular *n*-alkanes, reaching nearly –8 per mille (Ruhl *et al.* 2011). In contrast, marine bulk organic (Bachan *et al.* 2012) and carbonate carbon records often show no excursions or else much smaller negative excursions (Galli *et al.* 2005). A major positive CIE in bulk carbonate that follows the end-Triassic extinction event in the Southern Alps and the Apennines (Italy; van de Schootbrugge *et al.* 2008; Bachan *et al.* 2012) is missing from marine bulk organic (Ruhl *et al.* 2010) and terrestrial compound-specific carbon isotopes (Whiteside *et al.* 2010), preventing a complete understanding of Triassic–Jurassic carbon cycle dynamics.

Following a major episode of flood basalt eruption, carbon dioxide build-up in the atmosphere lasted for at least 30 ka before silicate weathering and organic carbon burial led to remediation of excess carbon (Archer 2005; Bachan & Payne, 2015). The immediate result, and a proximate kill mechanism for many benthic and planktonic calcareous organisms, was ocean acidification combined with global greenhouse warming. Ocean acidification would only be effective if the injection of volcanic volatiles was rapid, of the order 10 ka or less (Bachan & Payne, 2015). Strong greenhouse warming due to the emission of volcanic CO_2 has been inferred based on a number of proxy records from Permian–Triassic and Triassic–Jurassic boundary beds.

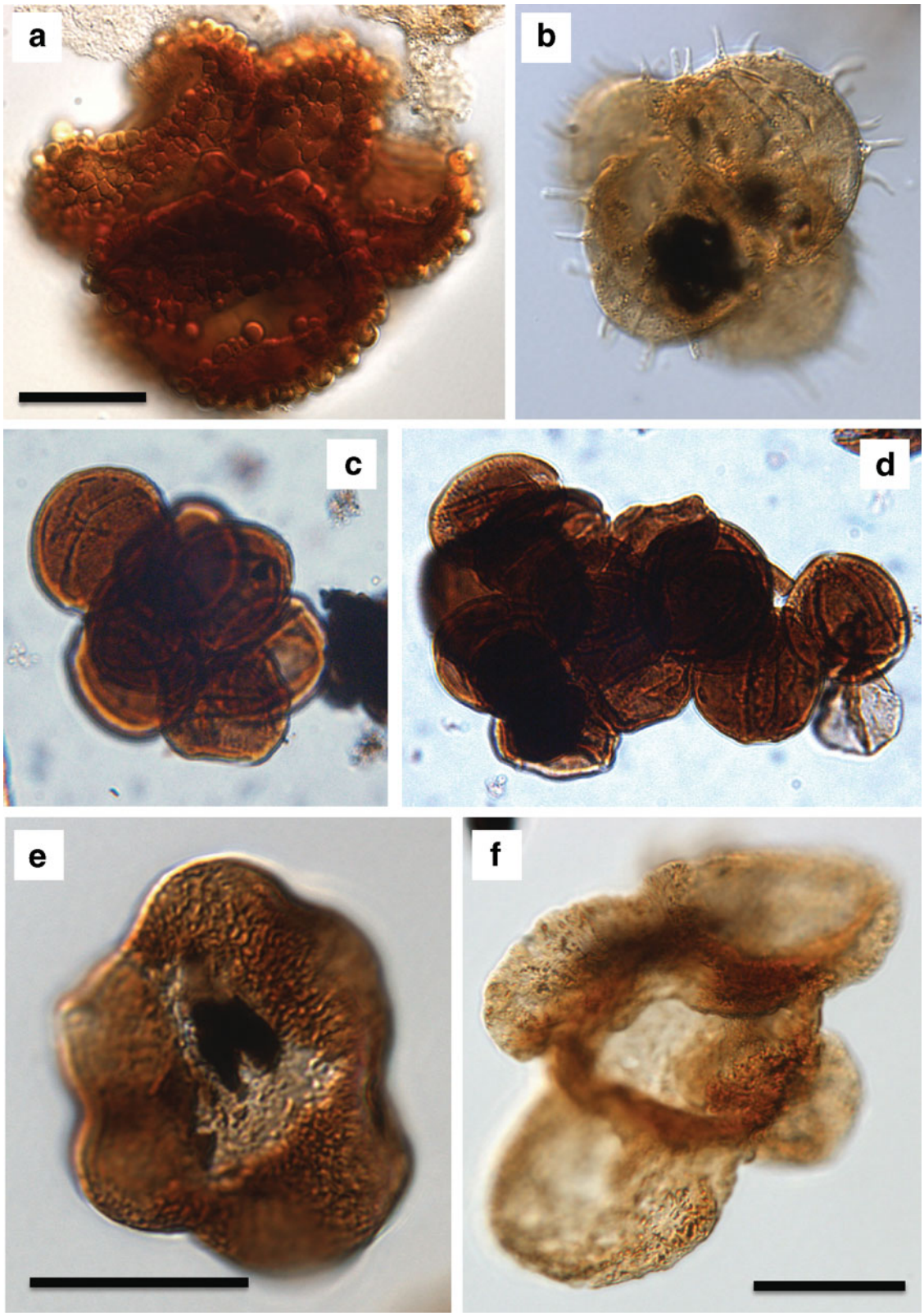

Figure 3. (Colour online) Aberrant pollen and spores from the end-Triassic extinction interval (scale bars are 20 μm). (a) *Ricciisporites tuberculatus* from the uppermost Rhaetian deposits at Larne (Northern Ireland). This enigmatic gymnosperm pollen that has distinct and highly variable surface ornamentation became one of the major victims of the ETME. (b) *Kraeuselisporites reissingerii* from the lowermost Hettangian deposits of Larne. These lycopsid spore-tetrads proliferate in the direct aftermath of the end-Triassic extinction, similar to that observed for the end-Permian mass extinction. The unseparated tetrads are possibly reflecting increased environmental stress. (c, d) *Classopollis torosus* tetrads from the lowermost Hettangian deposits in the Schandelah-1 core from north Germany. These unseparated tetrads consisting of more than 4 pollen grains likely reflect an environmental stress response. Unreduced (polyploid) *Classopollis*-tetrads have been interpreted by (Kürschner, Batenburg & Mander, 2013) to explain the success of cheirolepid conifers following the ETME. (e) Trisaccate version of a normally bisaccate *Vitreisporites pallidus* from Rhaetian sediments in the Schandelah-1 core. (f) Quadrisaccate version of a normally bisaccate pollen grain related to *Pinuspollenites minimus* from the lowermost Hettangian section in the Rosswinkel core from Luxemburg.

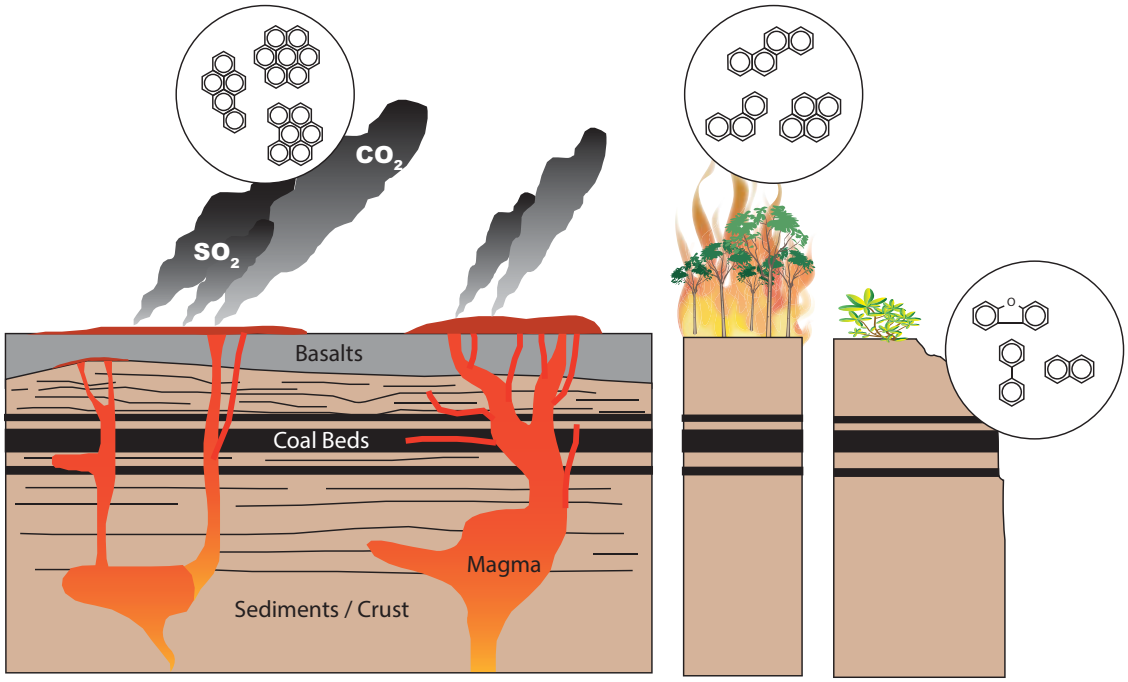

Figure 4. (Colour online) Conceptual framework to explain the abundance of high-molecular-weight and low-molecular-weight PAHs in boundary strata from the end-Permian and end-Triassic extinction events. The HMW compounds are generated via high-temperature charring of organic matter, coals or hydrocarbons during LIP emplacement. LMW compounds are generated via forest fires and weathering of soils.

However, direct evidence for elevated pCO_2 for the end-Permian extinction is relatively scarce and mostly relies on carbon cycle modelling and carbon isotope records (Fraiser & Bottjer, 2007). Retallack (2013) sees evidence for multiple greenhouse crises based on the occurrence of palaeosols that recorded hot and dry spells during late Permian – Early Triassic time. In contrast, detailed palynological records from Permian–Triassic sections in Pakistan revealing the variations in pollen and spores, in particular the occurrence of a single spore spike, suggest only one episode of particularly humid conditions during earliest Triassic time (Hermann *et al.* 2011).

A number of recent studies make a strong case for both increases in pCO_2 and warming associated with the Triassic–Jurassic boundary. At least four pulses of pCO_2 increase have been reconstructed using carbonate carbon isotope records measured on pedogenic carbonate nodules from continental sections in the Newark Basin (Schaller, Wright & Kent, 2011). Pedogenic carbonates from the Hartford Basin indicate CO_2 levels may have risen to nearly 5000 ppm during earliest Jurassic time, a doubling from latest Triassic values (Schaller *et al.* 2012). Plants are sensitive recorders of atmospheric CO_2 via stomatal density and size, and leaf stomata indicate a strong increase in atmospheric pCO_2 during earliest Jurassic time from 1000 ppm to 2000–3000 ppm (McElwain, Beerling & Woodward, 1999; Steinthorsdottir, Jeram & McElwain, 2011). Evidence for greenhouse warming across the end-Triassic extinction has also been determined using pollen and spore records (Bonis, Ruhl & Kürschner, 2010). The strong increase in the cheirolepidacean pollen taxon *Classopollis* during earliest Hettangian time, produced by an extinct, presumed thermophilic, group of conifers, is seen as reflecting higher temperatures and more arid conditions. Such interpretations of pollen records are in line with modelling exercises using coupled ocean–atmosphere climate models. Huynh & Poulsen (2005) have demonstrated how a four-fold increase in pCO_2 can cause an increase in the severity and number of hot days and days without precipitation, as well as enhanced seasonality.

3. The continents

3.a. Pathogens

Forest dieback was both a consequence and potentially a cause of the end-Permian and end-Triassic extinction events. Loss of vegetation cover can trigger secondary extinctions among herbivores, particularly insects and herbivorous reptiles (Roopnarine, 2006). In addition, deforestation leading to extreme fragmentation of forested landscapes can lead to further extinction, as shown for example by a survey of extinction rates among small mammals in a Thai tropical forest (Gibson *et al.* 2013). Forest fragmentation has been claimed as a major factor in driving secondary extinctions in herbivorous reptiles across the end-Permian extinction (Benton & Newell, 2014).

Palynological records from across Europe provide evidence for complete loss of tree-bearing vegetation reflected in a strong decline in pollen abundance at the end of the Triassic. In several locations (notably in North Germany), typical dominant Rhaetian

pollen taxa including *Ovalipollis*, *Rhaetipollis*, *Ricciisporites* and *Classopollis*, disappear completely from upper Rhaetian assemblages (van de Schootbrugge *et al.* 2009; Heunisch *et al.* 2010), recording the loss of tree-bearing vegetation. This was accompanied by the spread of ferns and fern allies, including horsetails, which likely represent hardy taxa that were able to cope with adverse conditions during latest Rhaetian time. In this interval the dominant spore taxon *Polypodiisporites polymicroforatus*, that makes up 35 % of the palynomorph assemblages in Germany and Denmark, most likely derives from a schizaeaceous fern that bears all the hallmarks of a true pioneering species as it occurs in low frequencies in lower Rhaetian assemblages prior to the environmental changes. Such behaviour is typical for opportunistic early successional species that do well in the background, but thrive during ecosystem collapse.

Heat stress has been suggested as a factor in a 95 % turnover in Late Triassic plant species in eastern Greenland (McElwain, Beerling & Woodward, 1999). However, global drying due to extreme hothouse conditions contradicts the success of ferns and fern allies following the end-Permian and end-Triassic extinction events. The spread of a fern-dominated vegetation was consistent with an increase in seasonality, perhaps with brief periods of extreme rainfall alternating with longer dry spells. Analysis of palaeosol-types across the Permian–Triassic boundary appears to provide evidence for such a scenario (Retallack, 2013). However, it remains unclear how climate change triggered the extinction of entire plant groups – including the disappearance of the Permian Southern Hemisphere glossopterids and cordaites, arguably two groups of plants with very different ecological preferences – or the extinction of the peltasperms during the end-Triassic event.

Stress, for example due to climate change leading to drought or frost damage, is unlikely to have been a direct cause driving the extinction of land plants. However, stress does make plants more susceptible to infection with pathogens (Wargo, 1996). Moreover, elevated global temperatures can lead to increased virulence of plant pathogens, particularly of fungi (Fig. 5). As for their host plants, fungal pathogens adapt to fluctuations in temperature, humidity and seasonality (Yáñez-López 2012) and rising temperatures will extend the geographic range of most pathogens into higher latitudes (Chakraborty, Tiedemann & Teng, 2000). Fungi have been implicated in the end-Permian extinction based on the widespread occurrence of the palynomorph *Reduviasporonites* in Permian–Triassic boundary sediments (Eshet, Rampino & Visscher, 1995; Visscher *et al.* 1996; Steiner *et al.* 2003). Initially interpreted as the remains of saprotrophic (wood-decaying) fungi (Visscher *et al.* 1996), *Reduviasporonites* has recently been re-interpreted as the remains of a soil-borne pathogen similar to the extant *Rhizoctonia* (Visscher, Sephton & Looy, 2011). Today, this globally occurring fungal species causes root rot in a large number of different host species.

Some authors have questioned the role of *Reduviasporonites* in the end-Permian extinction, based on the low abundance of the fungal hyphae in high-latitude sections in Greenland and Norway (Hochuli *et al.* 2010); however, low abundance or even absence are to be expected considering the optimal thermal tolerance of pathogenic fungi (Yáñez-López 2012; Fig. 6). Such an optimal tolerance of the fungi in warmer climates is fully consistent with the very high abundances of *Reduviasporonites* in low-latitude sites in Italy (Visscher *et al.* 1996), Israel (Eshet, Rampino & Visscher, 1995) and the Karoo (Steiner *et al.* 2003).

It is not only plants which are sensitive to diseases; vertebrate populations can also be decimated by diseases. Well-known examples are the ravaging of Tasmanian devil populations (decline is of the order 70 %) by the spread of a facial tumour disease caused by a parasitic cancer (Siddle *et al.* 2007). A parasitic fungus killing frogs worldwide is another telling example. Although it needs to be stressed that amphibians appear not to have been the main victims of either the end-Permian or end-Triassic extinctions, amphibians might be the first group of organisms to suffer from the ongoing 'sixth' mass extinction (Wake & Vredenburg, 2008). Global populations of amphibians are currently threatened by single fungal pathogen *Batrachochytrium dendrobatidis* (*Bd*). This fungus has in some cases led to the extirpation of entire species in less than 2 years and it is feared 30 % of all 6300 amphibian species could fall victim to this single pathogen (Wake & Vredenburg, 2008). In addition, a related fungus *B. salamandrivorans* is threatening mainly salamanders and newts across Europe (Martel *et al.* 2014). The strongly increased global incidence of skin-infecting *Bd* since 1998 has been related to global warming, although some authors argue that a lack of data does not allow such a link to be made (Rohr *et al.* 2008).

3.b. Fire

Forest fires are an unlikely proximate extinction mechanism because many plants prosper after burning, while some need fire to germinate. Increased incidence of forest fires during mass-extinction events are likely a reflection of important changes in climate, for example increased storminess, leading to more lightning strikes, and longer dry spells (Belcher *et al.* 2010). Pyrofusinite, a vague term to describe charcoalified wood particles in coal petrology studies, has been detected in charcoal layers in proximity to the end-Permian extinction horizon in a number of sections across southern China (Shen *et al.* 2011*a*). In addition, the high abundance of polycyclic aromatic hydrocarbons (PAHs) in core material from Australia and outcrops in China and Canada has also been used to infer widespread forest fire activity during latest Permian time (Grice, Nabbefeld & Maslen, 2007; Nabbefeld *et al.* 2010). PAH concentrations follow fluctuations in black carbon particles with preserved wood structures in the GSSP section at Meishan, indicating a link between

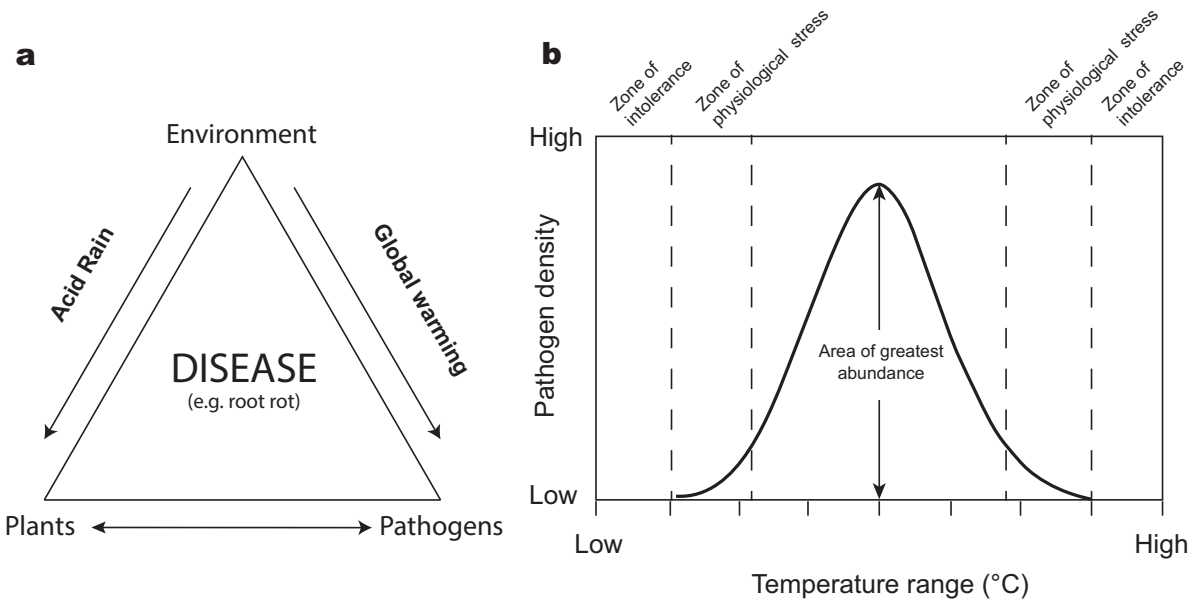

Figure 5. (a) Disease triangle, a conceptual framework introduced by Stevens (1960) to explain interactions between the environment, pathogens and plants in driving disease. Environmental changes influence both pathogens and plants. For example, acid rain may weaken the immune defence of plants, while at the same time warming may lead to increased virulence of pathogens (e.g. root rot fungi). Together these factors drive increased risk of infection and disease as a proximate kill mechanism. (b) Tolerance curve as a function of temperature for pathogenic fungi (modified from Yáñez-López, 2012) showing optimal range and absence in regions with exceptionally low (high latitudes) and/or high temperatures (low latitudes).

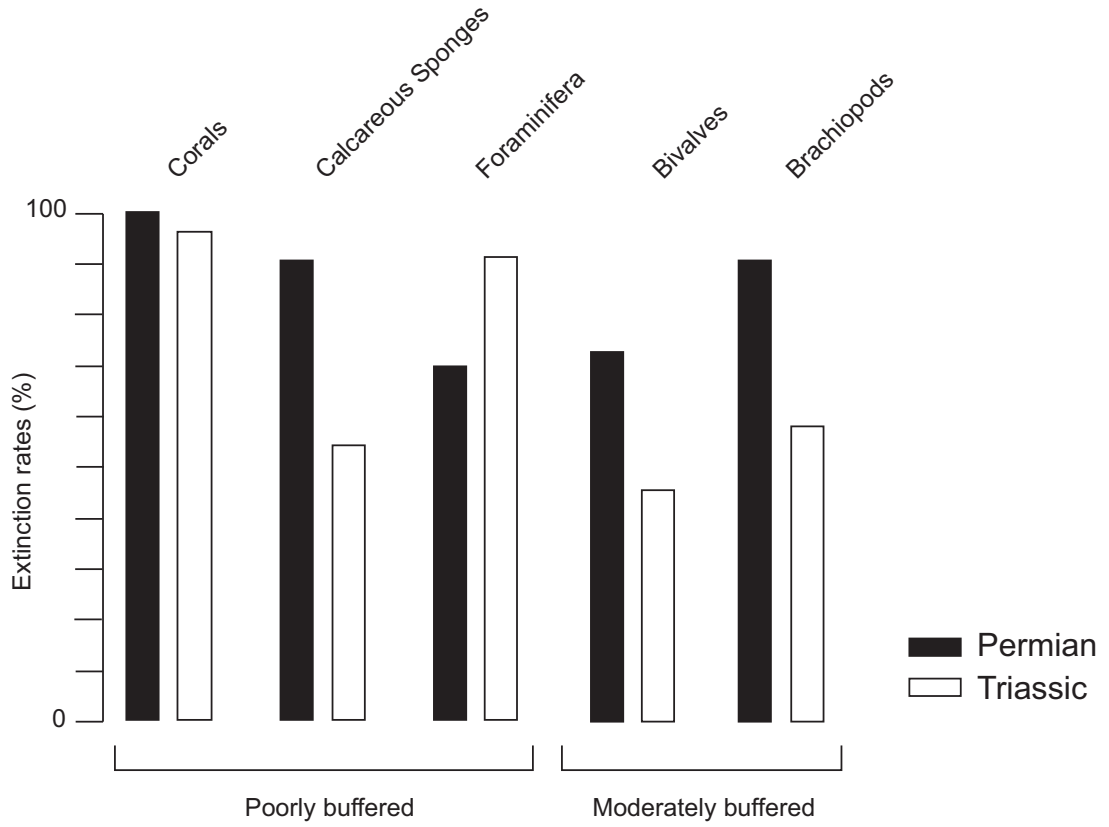

Figure 6. Comparison of extinction rates for poorly buffered and moderately buffered groups of calcareous organisms during the end-Permian (modified from Payne & Clapham, 2012) and end-Triassic extinction events (Hautmann, Benton & Tomasovych, 2008). Cnidarians were among the hardest-hit groups in both extinction events, leading to prolonged periods without significant reef build-ups (‘reef gaps’).

PAH and forest fire activity (Shen *et al.* 2011*b*). At Meishan the most dominant PAH are the 3- and 4-ring unsubstituted PAHs such as phenantrene, chrysene and benzo(e)pyrene, while the HMW PAHs (including coronene) occur in very low abundance. A volcanic link for fly-ash occurrences in Arctic Canada (Grasby, Sanei & Beauchamp, 2011) has recently been called into question by Hudspith, Rimmer & Belcher (2014) based on observations that peat-burning can also produce similar vesiculated chars. It should however be stressed that massive flood basalt volcanism producing pyrogenic substances (PAH, soot) does not exclude the simultaneous raging of forest fires; in some instances, volcanism is in fact the likely trigger for widespread forest fires.

Increased burning of vegetation has also been implicated in the end-Triassic extinction based on high abundances of charcoal in Greenland (Belcher *et al.* 2010), Germany (Uhl & Montenari, 2011) and Poland (Marynowski & Simoneit, 2009). Charcoal abundance in Greenland is coupled to elevated concentrations of PAH, particularly retene, which shows a single spike at the locally defined Triassic–Jurassic boundary (between plant beds 5a and 5b). Interestingly, low charcoal abundance in plant bed 4 correlates with high amounts of the HMW compounds coronene and benzo(*g,h,i*)perylene (Williford *et al.* 2014). Similar mismatches between charcoal abundance and the presence of pyrogenic PAHs have been observed in Poland (Marynowski & Simoneit, 2009) where some beds with high PAH do not contain charcoal. What is clear is that beds with high charcoal abundance mainly contain elevated concentrations of dibenzofurans and 3- and 4-ring PAH of pyrolytic origin.

3.c. Weathering and erosion

Acid rain, elevated pCO_2, increased seasonality and reduced plant cover all conspired to substantially increase weathering and erosion on the continents across the end-Permian and end-Triassic extinctions. Furthermore, forest fires count among the most effective ecological disturbance, leading to strongly enhanced mass-wasting and erosion as a result of the stripping of vegetation. Changes in river systems from meandering to anastomosing as observed in the Karoo Basin (South Africa; Ward, Montgomery & Smith, 2000) may provide evidence for a strong increase in rainfall and bed load, coeval with a dieback in tree-forming vegetation. More detailed sedimentological investigations, paired with vertebrate palaeontology, however suggests that droughts prevailed during earliest Triassic time in the Karoo (Smith & Botha-Brink, 2014). Perhaps the stripping of vegetation was the key in this setting to alter river morphology. Elsewhere, in the Ural Mountains and on the Russian Platform, the late Permian Period witnessed the abrupt arrival of coarse siliciclastics on top of muddy floodplain sediments (Newell *et al.* 2010). Increased transfer from continents to oceans seems apparent in a seven-fold increase in siliciclastic sedimentation rates that have been determined from well-dated sections in China (Algeo & Twitchett, 2010). Smothering has been invoked as an additional disturbance during the end-Permian extinction on epi- and infaunal marine invertebrate communities (Algeo & Twitchett, 2010).

A strong increase in woody material (phytoclasts) in Permian–Triassic boundary sections in the Italian Dolomites has been interpreted as evidence for forest dieback and increased erosion of soils (Visscher *et al.* 1996). Boundary clays contain abundant low-molecular-weight PAHs, such as alkylated napthalenes and benzofurans, interpreted as evidence of increased input of degraded plant material (polysaccharides) (Sephton *et al.* 1999, 2005; Watson *et al.* 2005). Alternatively, these PAHs were directly sourced by forest fires or volcanism, or may be diagenetic products of higher-molecular-weight PAHs. In all cases, they most likely represent increased soil erosion on the continents.

There is little information about changes in river morphology before and/or after the end-Triassic extinction. In the North German Basin, Upper Triassic deposits contain a series of massive sandstone beds that represent regional marker horizons. The upper Rhaetian Exter Formation, which also includes the extinction interval recorded in the fine-grained Triletes Beds, contains a massive coarse-grained sandstone at its base. Similar coarse-grained sandstones are known from Denmark and Sweden (Lindström *et al.* 2012). There is clear evidence for increased chemical weathering rates during late Rhaetian time from the occurrence of the clay mineral kaolinite in boundary beds. In the German Basin, the Triletes Beds show an enrichment in kaolinite relative to illite (van de Schootbrugge *et al.* 2009), and elevated abundance of kaolinite in boundary beds has been documented in Austria (Zajzon *et al.* 2012) and Poland (Pienkowski, Niedzwiedzki & Branski, 2014). Chemical weathering rates appear to have remained high, as the clay mineral assemblage in the Hettangian Blue Lias Formation in the UK continues to show abundant kaolinite (Deconinck *et al.* 2003).

4. The oceans

4.a. Changes in ocean temperature

Due to strengthened greenhouse climate conditions across the Permian–Triassic and Triassic–Jurassic boundaries, ocean temperatures may have risen to lethal levels (Sun *et al.* 2012; Song *et al.* 2014). Surface water temperatures have been reconstructed from oxygen isotope records derived from conodont apatite in China and Iran (Sun *et al.* 2012; Schobben *et al.* 2014). In equatorial waters, temperatures rose by an astounding 15 °C from 21 to 36 °C during the earliest Triassic Griesbachian Stage (a period of only 800 ka). A slight cooling during Dienerian time was followed by further warming during late Smithian time, when

equatorial sea-surface temperatures may have exceeded 40 °C (Sun *et al.* 2012). Such temperatures can be regarded as lethal for many marine organisms, especially cephalopods and marine reptiles that have high oxygen demands at high temperatures. High ocean water temperatures are also thought to explain dwarfism (the 'Lilliput' effect) observed in many groups of organisms inhabiting equatorial waters across the Permian–Triassic boundary (Sun *et al.* 2012). Interestingly, oxygen isotopes from conodonts track the bulk carbonate carbon isotope record from the Nanpanjiang Basin (China), showing a near-perfect match between negative C-isotope excursions; this is suggestive of a massive release of isotopically light CO_2 and warming episodes.

A dramatic rise in temperatures has also been observed for the end-Triassic extinction, although the data density is less than for the Permo-Triassic interval. Conodonts became both rare and extremely small during latest Triassic time, which makes them less suited for measuring oxygen isotopes. More importantly, conodonts count as one of the rare animal groups to experience 100 % extinction at the end of Triassic time. Belemnite rostra, the preferred skeletal calcite for obtaining Mesozoic palaeotemperatures, only become abundant during Sinemurian time, well after the extinction event. Some records have been published that use oyster calcite as an archive of temperature changes (van de Schootbrugge *et al.* 2007; Korte *et al.* 2009), but both studies derive from small and fairly restricted basins in the UK. Nonetheless, the oyster calcite oxygen isotope records from Lavernock Point, St Audrie's Bay and Lyme Regis document a 10 °C rise in sea-surface temperatures from latest Triassic – earliest Jurassic time (Korte *et al.* 2009). Interestingly, the oxygen isotope record from Lavernock Point follows the bulk carbonate carbon isotope record, providing further evidence for a coupling between temperature changes and the global carbon cycle. Temperatures appear to have stabilized around early–late Hettangian time.

4.b. Marine anoxia

Ocean de-oxygenation and the spread of 'dead zones' is a major threat to oceans and marine life today. 'Dead zones', such as those which develop each year in the Gulf of Mexico (Diaz & Rosenberg, 2008), result from a combination of factors including enhanced runoff, triggering both salinity stratification as well as eutrophication which then leads to enhanced primary production (Murphy, Kemp & Ball, 2011). Ultimately, the sinking of dead algal matter drives excess oxygen consumption in bottom waters. Both the end-Permian and end-Triassic extinction events were associated with widespread anoxic to euxinic conditions (Hallam & Wignall, 1997). Initially, dysoxia was recognized mainly from sedimentological and petrographic observations of laminated, pyritic and organic-rich sediments in Tethyan sections, for example in the Italian Dolomites (Wignall & Hallam, 1992; Twitchett, 1999). In Japan, the end-Permian extinction was marked by the replacement of red, radiolarian cherts with pyritic, black shales and siliceous mudstones that persist until the Middle Triassic (Isozaki, 1997; Wignall *et al.* 2010; Algeo *et al.* 2011).

During the climactic phase of the end-Permian extinction, dysoxic conditions intensified globally (Wignall & Twitchett, 2002; Bond & Wignall, 2010) and in some places photic zone euxinia developed, that is, a photic zone saturated in hydrogen sulphide. Biomarkers for green sulphur bacteria, photosynthetic lithotrophs that need H_2S and light, have been detected in boundary shales in Meishan (China; Cao *et al.* 2009), Australia (Grice *et al.* 2005*a*) and in outcrops and cores from western Canada (Hays *et al.* 2007). Shallowing of euxinia from the seafloor into the water column has also been inferred from the size of pyrite framboids (Wignall, Newton & Brookfield, 2005; Shen *et al.* 2007), as well as positive excursions in carbonate-associated sulphur (CAS) isotopes (Kampschulte & Strauss, 2004; Riccardi, Arthur & Kump, 2006). Positive excursions in CAS isotopes have been explained by strongly increased pyrite burial whereby bacterial sulphate reduction leads to removal of ^{32}S, leaving the residual sulphate reservoir enriched in the heavy ^{34}S (Newton *et al.* 2004). In places where anoxia was not strongly developed, such as in Oman, the recovery of benthic ecosystems proceeded at a higher pace, suggesting that prolonged anoxic conditions in shallow seas contributed to the overall slow recovery rates (Twitchett *et al.* 2004).

Remarkably little is known about the end-Triassic sulphur cycle. What is known is that anoxic conditions started to become prevalent in basins bordering the Tethys Ocean as early as during Rhaetian time. Thick black shales accumulated during late Rhaetian time in the Lago Negro Basin in southern Italy (Ciarapica, 2007) and local basins in Austria, such as the Kössen and Eiberg basins, also contain late Rhaetian organic-rich shales alternating with limestones (Holstein, 2004). Similar to that observed for the end-Permian event, euxinic conditions then spread into shallow epicontinental seaways across NW Europe during earliest Hettangian time (although this was after the mass extinction) (Hallam, 1995). High concentrations of isorenieratane, a carotenoid biomarker specific for green sulphur bacteria, occur in basal Jurassic black shales in Germany, Luxemburg and the UK (Richoz *et al.* 2012; Jaraula *et al.* 2013). Even though biomarkers cannot be detected in each section with black shales, due to issues with diagenesis and maturity of the sediments, syngenetic pyrite framboids also point to euxinia in Canada and England (Wignall *et al.* 2007; Wignall & Bond, 2008). Few Triassic–Jurassic sulphur isotope records exist that may underpin chemocline excursions, but a large positive excursion in bulk sulphur isotope values has been interpreted as reflecting intensified sulphate reduction in the Panthalassa Ocean (Williford *et al.* 2009) even though there is no sedimentary or petrographic evidence for ocean floor anoxia in the Panthalassa Ocean in Japan (Hori *et al.* 2007; Wignall

et al. 2010). Sulphate reduction may have been occurring within a mid-water oxygen minimum zone.

The release of H_2S to the atmosphere from euxinic waters has been advocated as an additional mechanism to lead to build-up of SO_2 in the atmosphere during the end-Permian extinction (Kump, Pavlov & Arthur, 2005). However, model calculations show such a mechanism would require the development of euxinia in large parts of the Tethys and Panthalassa oceans, as well as repeated overturn of deep water (Harfoot, Pyle & Beerling, 2008). The spread of euxinic conditions was likely spatially complex and may have been limited to shallow seas during latest Triassic time, although some recent evidence from Haida Gwaii (western Canada) suggest that open ocean sites in the Panthalassa were also euxinic (Kasprak *et al.* 2015). Anoxia had not developed everywhere at the time of the Triassic–Jurassic boundary; no evidence for anoxia has been found in Tibet, for example (Hallam *et al.* 2000). In addition, in both deep-water and shallower Tethyan sections, such as in Italy (Galli *et al.* 2005, 2007) and Montenegro (Crne *et al.* 2010), boundary clays are not particularly organic rich.

As pointed out by Payne & Clapham (2012), sustained anoxic to euxinic conditions following the end-Permian extinction would only be possible if surface waters became eutrophied, driving high rates of primary productivity (Meyer & Kump, 2008*a*; Meyer, Kump & Ridgwell, 2008; Meyer *et al*. 2011). An increased gradient in organic carbon isotope records along a margin to basin transect has been taken as evidence for an enhanced biological pump governing Early Triassic oceans (Meyer *et al.* 2011). The end-Permian extinction is also associated with the appearance of abundant acritarch and prasinophyte remains in sections worldwide from Greenland to Australia (Grice *et al.* 2005*b*). Although no carbon isotope transects exist for the end-Triassic extinction, changes in phytoplankton from dinoflagellate-dominated assemblages to assemblages dominated by acritarchs and prasinophytes are apparent (Richoz *et al.* 2012; van de Schootbrugge *et al.* 2013).

4.c. Acidification

As a result of unabated CO_2 emissions from fossil fuel burning, ocean pH is set to decline from 8.2 to 7.8 by the end of the current century (IPCC, 2014). Ocean acidification is increasingly seen as a major threat to the health of benthic and planktonic ecosystems in the oceans today. Aragonitic scleractinian corals, and therefore entire reefs, are predicted to be at risk in particular (Hoegh-Guldberg *et al.* 2007). Ocean acidification has been suggested as having caused the extinction of heavily calcified organisms with poor buffering capacities, including rugose, tabulate and scleractinian corals, brachiopods and bivalves, during both the end-Permian (Knoll *et al.* 2007) and end-Triassic extinction events (Greene *et al.* 2012*b*), although supporting geochemical evidence is enigmatic.

Boron isotope records, obtained from bulk carbonates sampled in Oman, provide no evidence for acidification during the end-Permian mass extinction but instead reveal a brief (*c.* 10 ka) excursion suggestive of acidification during Early Triassic time, which may be implicated with later extinction losses (Clarkson *et al.* 2015). Sedimentary evidence, in the form of a limestone truncation surface seen in uppermost Permian deposits in Turkey, has been ascribed to short-term under-saturation leading to dissolution (Fig. 7). Payne *et al.* (2007) advocated this as evidence for acidification, although others see evidence here for an emergence surface (Wignall & Bond, 2008). Newly emerged evidence from the Nanpanjiang Basin in China suggests that submarine dissolution may have been more widespread (Lehrmann *et al.* 2015). However, these sedimentary clues considerably pre-date the B-isotope evidence for acidification.

The most characteristic attribute of carbonate platforms during the Permo-Triassic interval is the presence of stromatolitic or thrombolitic build-ups as seen in Turkey (Baud, Richoz & Marcoux, 2005) and China (Kershaw, Zhang & Lan, 1999), suggesting supersaturation. Strongly supersaturated seawaters during Early Triassic time are also reflected by the deposition of syngenetic carbonates in the form of aragonite fans (Woods *et al.* 1999). An abundance of seafloor cements has been noted in Hettangian carbonate platform sections exposed in the Southern Alps (Italy) by Jadoul & Galli (2008) and linked to changes in saturation state. Further south in the Italian Apennines, massive cements and tepee-structures characterize much of the Lower Jurassic deposits (Fig. 7). The occurrence of crystal fans in the Fernie Formation in Canada has also been advocated as evidence for changes in ocean pH (Greene *et al.* 2012*a*), although these latter occurrences resemble late diagenesis 'beef calcite' which has recently been linked to the generation of hydrocarbons (Cobbold & Rodrigues, 2007; Cobbold *et al*. 2013). True aragonite fans were observed by Bachan *et al.* (2012) in the Southern Alps (Italy).

Ocean acidification is increasingly seen as a mechanism to explain the abrupt disappearance of reef ecosystems and more than 95 % extinction in scleractinian corals during latest Rhaetian time (Martindale *et al.* 2012). Sedimentological evidence for ocean acidification, such as the presence of carbonate-devoid boundary clays in both the Tethys and Panthalassa oceans, has been discussed by Hautmann, Benton & Tomasovych (2008). Abrupt changes in carbonate sedimentation are apparent in many sections bordering the Tethys Ocean in Italy and Greece (Bachan, van de Schootbrugge & Payne, 2014). The disappearance of reef organisms in the Zu Formation in the Val Adrara section (Italy) was also extremely abrupt; however, this may have been partly due to regression and erosion at the contact between the Zu Formation and the overlying Malanotte Formation. Trends in shell thickness have been used to argue against acidification across the ETME (Mander, Twitchett & Benton, 2008). Nevertheless, large

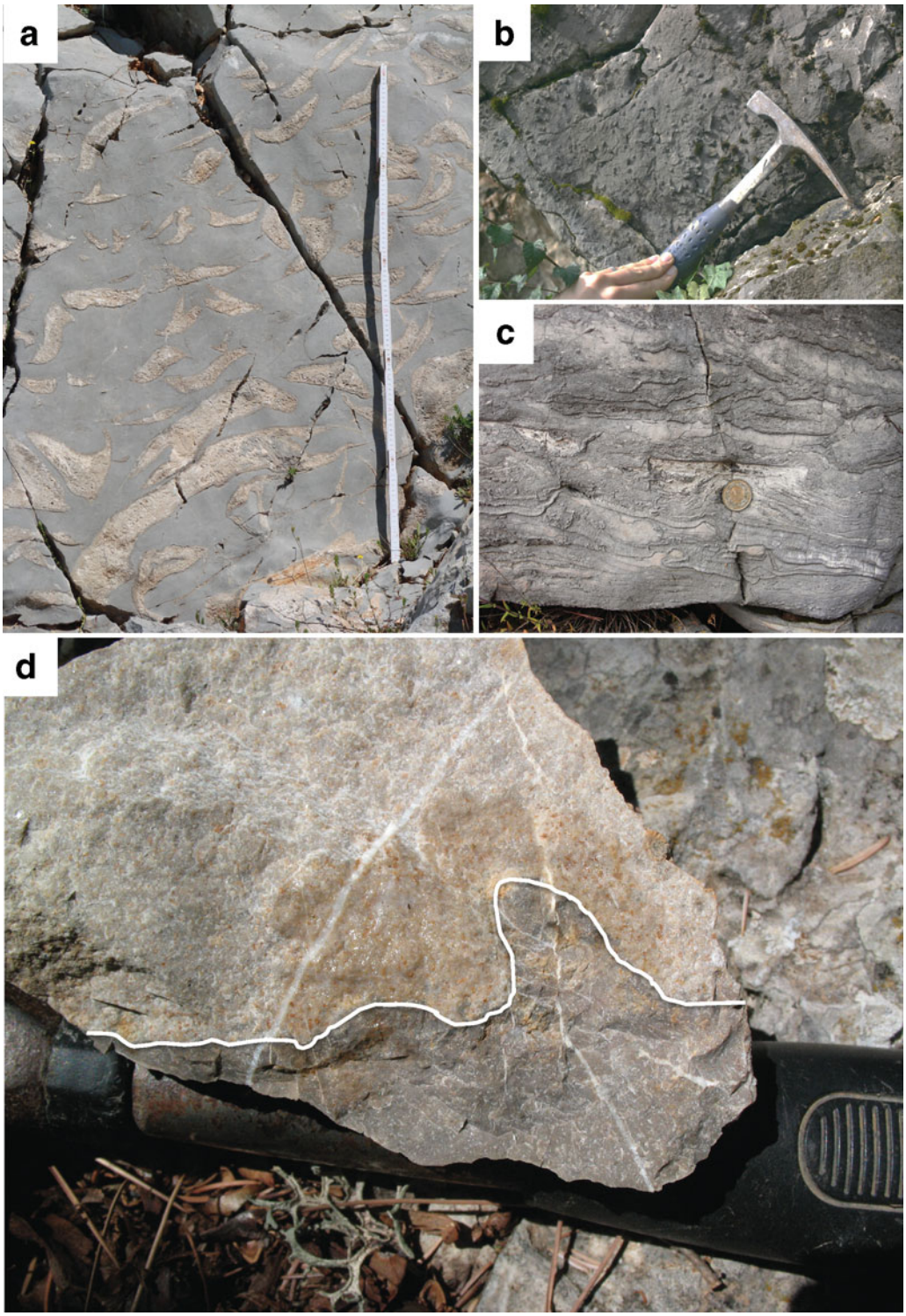

Figure 7. (Colour online) (a) Uppermost Rhaetian mudstones with giant megalodontid bivalves in the Mount Messapion section (Greece). These large bivalves abruptly disappear at the Triassic–Jurassic boundary (e.g. Romano *et al.* 2008), providing a dramatic example of a crisis in biocalcification during the ETME. (b) Topmost bed of the Rhaetian Zu Limestone Formation in the Val Adrara section (Southern Alps, Italy). This bed contains abundant recrystallized scleractinian corals and other bioclasts, and is abruptly overlain by thin-bedded limestones of the Malanotte Formation (see also Bachan *et al.* 2012 for lithological logs). (c) Abundant early diagenetic cements in the Hettangian Valle Agricola section (Apennines, Italy). Similar sedimentary features also characterize the Hettangian deposits further south in the Monte Cefalo section close to Naples (see Bachan *et al.* 2012), perhaps suggesting carbonate supersaturation in shallow oceans due to a breakdown in biological carbonate precipitation. (d) Photograph of the Permian–Triassic boundary bed in the Çürük Dag section in Turkey showing sharp irregular contact between a *Gymnocodium* packstone and a pelsparite.

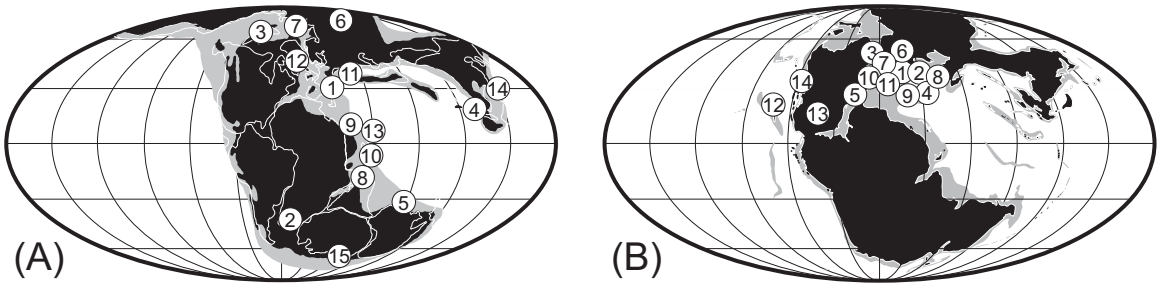

Proximate kill mechanism	End-Permian evidence for=	Locations* * see figure 8a	End-Triassic evidence for=	Locations* * see figure 8b
Atmosphere				
Acid rain	Some	*(1, 2)*	Circumstantial	*(1, 2)*
Elevated pCO_2	Circumstantial	*(15)*	Strong	*(3, 5)*
Pollution (e.g. Hg, PAH)	Strong	*(3, 4, 5, 6, 7)*	Some	*(1, 2)*
Thermogenic methane	Strong	*(6)*	Some	*(4, 5)*
Greenhouse warming	Strong	(5, 15)	Strong	*(3, 4, 5, 8, 10)*
Continents				
Forest fires	Strong	*(4, 5)*	Strong	*(1, 2, 3)*
Forest dieback	Strong	*(1, 2, 8, 16)*	Strong	*(1, 2, 3, 4, 5, 6, 7, 8, 10)*
Increased weathering	Some	*(2, 4)*	Strong	*(1, 2, 4, 5)*
Disease/mutations	Strong	*(1, 2, 4, 9)*	Some	*(1, 13)*
Oceans				
Acidification	Strong	*(10, 11)*	Circumstantial	*(9, 10)*
Photic zone euxinia/anoxia	Strong	*(4, 5, 7, 12, 14)*	Strong	*(1, 10, 11, 12, 14)*
Lethal hot temperatures	Strong	*(4, 13)*	Some	*(10)*

Figure 8. Comparison of proximate kill mechanisms for the end-Permian and end-Triassic extinction showing quality of evidence and locations where key evidence has been presented (non-exhaustive). (a) 1, Italy (Dolomites); 2, South Africa (Karoo Basin); 3, Canada (Sverdrup Basin); 4, China (Nanpanjiang Basin); 5, Australia; 6, Siberia (Tunguska Basin); 7, Svalbard; 8, Pakistan; 9, Israel; 10, Oman; 11, Turkey (Taurus Mountains); 12, Greenland; 13, Iran; 14, Japan; 15, Antarctica. (b) 1, Germany (north and south); 2, Poland; 3, Greenland; 4, Austria (GSSP and nearby sections); 5, United States (eastern); 6, Sweden (Scania); 7, Denmark; 8, Hungary; 9, Italy (Southern Alps, Apennines); 10, England (Somerset); 11, Luxemburg; 12, Canada (Haida Gwaii); 13, United States (southwest); 14, Canada (Williston Basin).

megalodontid bivalves in Tethyan shallow-marine carbonate platform sections in Italy and Greece not only disappeared abruptly, but the surviving faunas contained species that were strongly reduced in size (Hautmann, 2004). At Mount Messapion in a section close to Athens (Greece), the abrupt disappearance of the huge megalodontid bivalves is both puzzling and striking (Romano *et al.* 2008; Fig. 7). These bivalves may have grown to such large sizes because of the presence of photosymbionts, and their extinction and reduction in size could potentially have been triggered by disturbances in this symbiotic partnership.

5. Converging scenarios: similarities and differences

Scenarios for the end-Permian and end-Triassic extinction events are increasingly converging, and both are now commonly linked to the emplacement of the large igneous provinces of the Siberian Traps and the Central Atlantic Magmatic Province. Overall, the following scenario is relevant to both the end-Permian and end-Triassic extinction. Flood basalt volcanism released large quantities of sulphur dioxide, carbon dioxide, thermogenic methane and potentially large amounts of pollutants such as HF, HCl, halocarbons and toxic aromatics and heavy metals into the atmosphere. Volatile loads were likely exacerbated by country-rock – lava interactions depending on the intrusions of sills into organic-rich and/or evaporitic and petroleum-rich crustal rocks. The released volatiles exerted a range of influences on atmospheric chemistry, leading to tropospheric transport of pollutants and sulphuric acid aerosols and a potential breakdown in ozone concentrations in the stratosphere. Acid rain likely had an impact on freshwater ecosystems and may have triggered forest dieback, whereas increased UV radiation from decreased ozone shielding may have triggered malformations in plant reproductive systems. The stripping of vegetation due to environmental pollution and climate change, perhaps aided by repeated burning, greatly enhanced weathering and erosion rates, ultimately driving high nutrient input into shallow oceans. Eutrophication of surface waters drove high primary productivity and, coupled with high water temperatures, led to widespread anoxia and repeated photic zone euxinia.

These scenarios are supported by much of the reviewed literature and data; however, differences and strong similarities may be noted between the end-Permian and end-Triassic extinctions (Fig. 8). Such a comparison may give insight into scenarios that are

more strongly supported, and highlight our gaps in understanding. Overall, there is more global evidence for environmental change associated with the end-Permian extinction. There is clearly a lack of key evidence from the Southern Hemisphere for the end-Triassic extinction (Fig. 8). The end-Permian has also been studied more intensely, perhaps explaining a more global coverage. There is therefore some bias when comparing the extinction events. Nevertheless, strong evidence exists for anoxia and photic zone euxinia associated with both extinction events based on biomarkers, trace element records and pyrite framboids. On a more local scale charcoal records point to forest fires as a common denominator, while palynological and palaeobotanical evidence suggests that forest dieback was prevalent during both events. Together, these phenomena may have led to increased weathering and erosion on the continents, although the evidence collected so far for changes in clay mineral assemblages seems more robust for the end-Triassic extinction. While there is general consensus that both extinctions are also partly related to greenhouse warming, only direct evidence for a rise in pCO_2 (from stomata and pedogenic carbonates) comes from the end-Triassic extinction.

Acid rain remains difficult to demonstrate for both extinction events, and only very circumstantial evidence is available for the end-Triassic extinction. However, acid rain proxy records (sulphur isotopes in fresh water, biomarkers from soils) for the end-Permian extinction may equally be questioned. Other lines of evidence are generally more spurious for the end-Triassic extinction. Pollution with heavy metals or hydrocarbons is evident from a number of sites for the end-Permian extinction but, except for PAH records from Germany and Poland, such records are lacking for the end-Triassic. Evidence for severe stress (diseases, increased radiation) among primary producers from the abundance of fungal spores and mutated spores and pollen is clearer for the end-Permian extinction. However, recent findings of mutations in common Triassic pollen species close to the Triassic–Jurassic boundary in the United States should lead to more intense investigations of pollen and other records. In the oceans, evidence for acidification and lethal hot temperatures seems more abundant for the end-Permian extinction. This is partly due to a few easily accessible carbonate deposits or suitable calcitic micro- and macrofossils straddling the Triassic–Jurassic boundary that allow reconstructions of oxygen isotope records or other temperature proxy records. Both flood basalt provinces (Siberian Traps, CAMP) are situated in the Northern Hemisphere, and much can be learned from interhemispheric comparisons in order to understand the truly global impact of flood basalt eruptions. However, it is clear that more data are needed from the Southern Hemisphere for the end-Triassic extinction.

Acknowledgements. We thank Henk Visscher (Utrecht) for discussions and providing background information. Carolien van der Weijst (Utrecht) is thanked for providing pictures of palynomorphs. David Bond and an anynomous reviewer are thanked for their helpful comments that strengthened the final manuscript.

References

ALGEO, T. J., CHEN, Z. Q., FRAISER, M. L. & TWITCHETT, R. J. 2011. Terrestrial-marine teleconnections in the collapse and rebuilding of Early Triassic marine ecosystems. *Palaeogeography, Palaeoclimatology, Palaeoecology* **308**, 1–11.

ALGEO, T. J., KUWAHARA, K., SANO, H., BATES, S., LYONS, T., ELSWICK, E., HINNOV, L., ELLWOOD, B., MOSER, J. & MAYNARD, J. B. 2011. Spatial variation in sediment fluxes, redox conditions, and productivity in the Permian-Triassic Panthalassic Ocean. *Palaeogeography, Palaeoclimatology, Palaeoecology* **308**, 65–83.

ALGEO, T. J. & TWITCHETT, R. J. 2010. Anomalous Early Triassic sediment fluxes due to elevated weathering rates and their biological consequences. *Geology* **38**, 1023–6.

ARCHER, D. 2005. Fate of fossil fuel CO_2 in geologic time. *Journal of Geophysical Research* **110**, C09S05.

BACHAN, A. & PAYNE, J. L. 2015. Modelling the impact of pulsed CAMP volcanism on pCO_2 and $\delta^{13}C$ across the Triassic-Jurassic transition. *Geological Magazine*, published online 8 June 2015. doi: 10.1017/S0016756815000126.

BACHAN, A., VAN DE SCHOOTBRUGGE, B., FIEBIG, J., MCROBERTS, C. A., CIARAPICA, G. & PAYNE, J. L. 2012. Carbon cycle dynamics following the end-Triassic mass extinction: Constraints from paired $\delta^{13}C_{carb}$ and $\delta^{13}C_{org}$ records. *Geochemistry, Geophysics, Geosystems* **13**, Q09008.

BACHAN, A., VAN DE SCHOOTBRUGGE, B. & PAYNE, J. L. 2014. The end-Triassic negative $\delta^{13}C$ excursion: a lithologic test. *Palaeogeography, Palaeoclimatology, Palaeoecology* **412**, 177–86.

BAMBACH, R. K. 2006. Phanerozoic biodiversity mass extinctions. *Annual Review of Earth and Planetary Sciences* **34**, 127–55.

BARTIROMO, A., GUIGNARD, G., BARONE LUMAGA, M. R., BARATTOLO, F., CHIODINI, G., AVINO, R., GUERRIERO, G. & BARALE, G. 2012. Influence of volcanic gases on the epidermis of *Pinus halepensis* Mill. in Campi Flegrei, Southern Italy: A possible tool for detecting volcanism in present and past floras. *Journal of Volcanology and Geothermal Research* **233–234**, 1–17.

BASU, A. R., PETAEV, M. I., POREDA, R. J., JACOBSEN, S. B. & BECKER, L. 2003. Chondritic meteorite fragments associated with the Permian-Triassic boundary in Antarctica. *Science* **302**, 1388–92.

BAUD, A., RICHOZ, S. & MARCOUX, J. 2005. Calcimicrobial cap rocks from the basal Triassic units: western Taurus occurrences (SW Turkey). *Comptes Rendu Palevol* **4**, 501–14.

BECKER, L., POREDA, R. J., BASU, A. R., POPE, K. O., HARRISON, T. M., NICHOLSON, C. & IASKY, R. 2004. Bedout: a possible end-Permian impact crater offshore of northwestern Australia. *Science* **304**, 1469–76.

BECKER, L., POREDA, R. J., HUNT, A. G., BUNCH, T. E. & RAMPINO, M. 2001. Impact event at the Permian-Triassic boundary: Evidence from extraterrestrial noble gases in fullerenes. *Science* **291**, 1530–3.

BEERLING, D. J., HARFOOT, M., LOMAX, B. & PYLE, J. A. 2007. The stability of the stratospheric ozone layer during the end-Permian eruption of the Siberian Traps. *Philosophical Transactions of the Royal Society of*

London A: Mathematical, Physical and Engineering Sciences **365**, 1843–66.

BELCHER, C. M., MANDER, L., REIN, G., JERVIS, F. X., HAWORTH, M., HESSELBO, S. P., GLASSPOOL, I. J. & MCELWAIN, J. C. 2010. Increased fire risk associated with global warming across the Triassic–Jurassic boundary. *Nature Geoscience* **3**, 426–9.

BENTON, M. J. 1986. More than one event in the Late Triassic mass-extinction. *Nature* **321**, 857–61.

BENTON, M. J. & NEWELL, A. J. 2014. Impacts of global warming on Permo-Triassic terrestrial ecosystems. *Gondwana Research* **25**, 1308–37.

BENTON, M. J., TVERDOKHLEBOV, V. P. & SURKOV, M. V. 2004. Ecosystem remodelling among vertebrates at the Permian-Triassic boundary in Russia. *Nature* **432**, 97–100.

BENTON, M. J. & TWITCHETT, R. J. 2003. How to kill (almost) all life: the end-Permian extinction event. *Trends in Ecology and Evolution* **18**, 358–65.

BICE, D. M., NEWTON, C. R., MCCAULEY, S. E., REINERS, P. W. & MCROBERTS, C. A. 1992. Shocked quartz at the Triassic-Jurassic boundary in Italy. *Science* **255**, 443–6.

BLACK, B. A., LAMARQUE, J. F., SHIELDS, C. A., ELKINS-TANTON, L. T. & KIEHL, J. T. 2013. Acid rain and ozone depletion from pulsed Siberian Traps magmatism. *Geology* **42**, 67–70.

BLACKBURN, T. J., OLSEN, P. E., BOWRING, S. A., MCLEAN, N. M., KENT, D. V., PUFFER, J., MCHONE, G., RASBURY, E. T. & ET-TOUHAMI, M. 2013. Zircon U-Pb geochronology links the end-Triassic extinction with the Central Atlantic Magmatic Province. *Science* **340**, 941–4.

BÖHME, M., GREGOR, H.-J. & HEISSIG, K. 2002. The Ries and Steinheim meteorite impacts and their effect on the environmental conditions in time and space. In *Geological and Biological Effects of Impact Events* (eds F. Buffetaut & C. Koeberl), pp. 217–35. Heidelberg: Springer.

BOND, D. P. G. & WIGNALL, P. B. 2010. Pyrite framboid study of marine Permian-Triassic boundary sections: a complex anoxic event and its relationship to contemporaneous mass extinction. *Geological Society of America Bulletin* **122**, 1265–79.

BOND, D. P. G. & WIGNALL, P. B. 2014. Large igneous provinces and mass-extinctions: an update. In *Volcanism, Impacts, and Mass-Extinctions* (eds G. Keller & A. C. Kerr), pp. 30–56. Boulder: Geological Society of America.

BONIS, N. R., KÜRSCHNER, W. M. & KRYSTYN, L. 2009. A detailed palynological study of the Triassic-Jurassic transition in key sections of the Eiberg Basin (Northern Calcareous Alps, Austria). *Review of Palaeobotany and Palynology* **156**, 376–400.

BONIS, N. R., RUHL, M. & KÜRSCHNER, W. M. 2010. Milankovitch-scale palynological turnover across the Triassic-Jurassic transition at St Audrie´s Bay, SW UK. *Journal of the Geological Society of London* **167**, 877–88.

BOWRING, S. A., ERWIN, D. H., JIN, Y. G., MARTIN, M. W., DAVIDEK, K. & WANG, W. 1998. U/Pb zircon geochronology and tempo of the end-Permian mass extinction. *Science* **280**, 1039–45.

BRICKER, O. P. & RICE, K. C. 1993. Acid rain. *Annual Review of Earth and Planetary Sciences* **21**, 151–74.

BURGESS, S., BOWRING, S. & SHEN, S. Z. 2014. High-precision timeline for Earth's most severe extinction. *Proceedings of the National Academy of Science* **111**, 3316–21.

CALLEGARO, S., BAKER, D. R., DE MIN, A., MARZOLI, A., GERAKI, K., BETRAND, H., VITI, C. & NESTOLA, F. 2014. Microanalyses link sulfur from large igneous provinces and Mesozoic mass-extinctions. *Geology* **42**, 895–8.

CAO, C. Q., LOVE, G. D., HAYS, L. E., WANG, W. & SHEN, S. Z. 2009. Biogeochemical evidence for euxinic oceans and ecological disturbance presaging the end-Permian mass-extinction event. *Earth and Planetary Science Letters* **281**, 188–201.

CAO, H. 1989. Air pollution and its effects on plants in China. *Journal of Applied Ecology* **26**, 763–73.

CHAKRABORTY, S., TIEDEMANN, A. V. & TENG, P. S. 2000. Climate change: potential impact on plant diseases. *Environmental Pollution* **108**, 317–26.

CHENET, A.-L., FLUTEAU, F. & COURTILLOT, V. 2005. Modelling massive sulphate aerosol pollution, following the large 1783 Laki basaltic eruption. *Earth and Planetary Science Letters* **236**, 721–31.

CIARAPICA, G. 2007. Regional and global changes around the Triassic-Jurassic boundary reflected in the late Norian-Hettangian history of the Apennine basins. *Palaeogeography, Palaeoclimatology, Palaeoecology* **244**, 34–51.

CIRILLI, S., MARZOLI, A., TANNER, L., BERTRAND, H., BURATTI, N., JOURDAN, F., BELLIENI, G., KONTAK, D. & RENNE, P. R. 2009. Latest Triassic onset of the Central Atlantic Magmatic Province (CAMP) volcanism in the Fundy Basin (Nova Scotia): New stratigraphic constraints. *Earth and Planetary Science Letters* **286**, 514–25.

CLARKSON, M. O., KASEMANN, S. A., WOOD, R. A., LENTON, T. M., DAINES, S. J., RICHOZ, S., OHNEMUELLER, F., MEIXNER, A., POULTON, S. W. & TIPPER, E. T. 2015. Ocean acidification and the Permo-Triassic mass-extinction. *Science* **348**, 229–32.

COBBOLD, P. R. & RODRIGUES, N. 2007. Seepage forces, important factors in the formation of horizontal hydraulic fractures and bedding-parallel fibrous veins ('beef' and 'cone-in-cone'). *Geofluids* **7**, 313–22.

COBBOLD, P. R., ZANELLA, A., RODRIGUES, N. & LØSETH, H. 2013. Bedding-parallel fibrous veins (beef and cone-in-cone): Worldwide occurrence and possible significance in terms of fluid overpressure, hydrocarbon generation and mineralization. *Marine and Petroleum Geology* **43**, 1–20.

COURTILLOT, V. 1994. Mass extinctions in the last 300 million years: one impact and seven flood basalts. *Israel Journal of Earth Sciences* **43**, 255–66.

CRNE, A. E., WEISSERT, H., GORICAN, S. & BERNASCONI, S. M. 2010. A biocalcification crisis at the Triassic-Jurassic boundary recorded in the Budva Basin (Dinarides, Montenegro). *Geological Society of America Bulletin* **123**, 40–50.

DAL CORSO, J., MARZOLI, A., TATEO, F., JENKYNS, H. C., BERTRAND, H., YOUBI, N., MAHMOUDI, A., FONT, E., BURATTI, N. & CIRILLI, S. 2014. The dawn of CAMP volcanism and its bearing on the end-Triassic carbon cycle disruption. *Journal of the Geological Society of London* **171**, 153–64.

DECONINCK, J.-F., HESSELBO, S. P., DEBUISSER, N., AVERBUCH, O., BAUDIN, F. & BESSA, J. 2003. Environmental controls on clay mineralogy of an Early Jurassic mudrock (Blue Lias Formation, southern England). *International Journal of Earth Sciences* **92**, 255–66.

DIAZ, R. J. & ROSENBERG, R. 2008. Spreading dead zones and consequences for marine ecosystems. *Science* **321**, 926–9.

ELLIOTT-KINGSTON, C., HAWORTH, M. & MCELWAIN, J. C. 2014. Damage structures in leaf epidermis and cuticle as an indicator of elevated atmospheric sulphur dioxide

in early Mesozoic floras. *Review of Palaebotany and Palynology* **208**, 25–42.

ERWIN, D. H. 1993. *The Great Paleozoic Crisis: Life and Death in the Permian*. New York: Columbia University Press.

ESHET, Y., RAMPINO, M. R. & VISSCHER, H. 1995. Fungal event and palynological record of ecological crisis and recovery across the Permian-Triassic boundary. *Geology* **23**, 967–70.

EVANS, L. S. 1984. Acidic precipitation effects on terrestrial vegetation. *Annual Review of Phytopathology* **22**, 397–420.

FOSTER, C. B. & AFONIN, S. A. 2005. Abnormal pollen grains: an outcome of deteriorating atmospheric conditions around the Permian-Triassic boundary. *Journal of the Geological Society of London* **162**, 653–9.

FRAISER, M. L., BOTTJER, D. J. 2007. Elevated atmospheric CO_2 and the delayed biotic recovery from the end-Permian mass extinction. *Palaeogeography, Palaeoclimatology, Palaeoecology* **252**, 164–75.

GALLI, M. T., JADOUL, F., BERNASCONI, S. M., CIRIILI, S. & WEISSERT, H. 2007. Stratigraphy and palaeoenvironmental analysis of the Triassic-Jurassic transition in the western Southern Alps (Northern Italy). *Palaeogeography, Palaeoclimatology, Palaeoecology* **244**, 52–70.

GALLI, M. T., JADOUL, F., BERNASCONI, S. M. & WEISSERT, H. 2005. Anomalies in global carbon cycling and extinction at the Triassic/Jurassic boundary: evidence from a marine C-isotope record. *Palaeogeography, Palaeoclimatology, Palaeoecology* **216**, 203–14.

GANINO, C. & ARNDT, N. T. 2009. Climate changes caused by degassing of sediments during the emplacement of large igneous provinces. *Geology* **37**, 323–6.

GIBSON, L., LYNAM, A. J., BRADSHAW, C. J., HE, F., BICKFORD, D. P., WOODRUFF, D. S., BUMRUNGSRI, S. & LAURANCE, W. F. 2013. Near-complete extinction of native small mammal fauna 25 years after forest fragmentation. *Science* **341**, 1508–10.

GRASBY, S. E., BEAUCHAMP, B., BOND, D. P. G., WIGNALL, P. B. & SANEI, H. 2015. Mercury anomalies associated with three extinction events (Capitanian Crisis, Latest Permian Extinction and the Smithian/Spathian Extinction) in NW Pangea. *Geological Magazine*, published online 15 July 2015. doi: 10.1017/S0016756815000436.

GRASBY, S. E., SANEI, H. & BEAUCHAMP, B. 2011. Catastrophic dispersion of coal fly ash into oceans during the latest Permian extinction. *Nature Geoscience* **4**, 104–7.

GRATTAN, J. 2005. Pollution and paradigms: lessons from Icelandic volcanism for continental flood basalt studies. *Lithos* **79**, 343–53.

GREENE, S. E., BOTTJER, D. J., CORSETTI, F. A., BERELSON, W. M. & ZONNEVELD, J.-P. 2012*a*. A subseafloor carbonate factory across the Triassic-Jurassic transition. *Geology* **40**, 1043–6.

GREENE, S. E., MARTINDALE, R. C., RITTERBUSH, K. A., BOTTJER, D. J., CORSETTI, F. A. & BERELSON, W. M. 2012*b*. Recognising ocean acidification in deep time: an evaluation of the evidence for acidification across the Triassic-Jurassic boundary. *Earth Science Reviews* **113**, 72–93.

GRICE, K., CAO, C., LOVE, G. D., BÖTTCHER, M. E., TWITCHETT, R. J., GROSJEAN, E., SUMMONS, R. E., TURGEON, S. C., DUNNING, W. & JIN, Y. 2005*a*. Photic Zone Euxinia during the Permian-Triassic superanoxic event. *Science* **307**, 706–9.

GRICE, K., NABBEFELD, B. & MASLEN, E. 2007. Source and significance of selected Polycyclic Aromatic Hydrocarbons in sediments (Hovea-3 well, Perth Basin, Western Australia) spanning the Permian-Triassic boundary. *Organic Geochemistry* **38**, 1795–803.

GRICE, K., TWITCHETT, R. J., ALEXANDER, R., FOSTER, C. B. & LOOY, C. V. 2005*b*. A potential biomarker for the Permian-Triassic ecological crisis. *Earth and Planetary Science Letters* **236**, 315–21.

GUROV, E., GUROVA, E., CHERNENKO, Y. & YAMNICHENKO, A. 2009. The Obolon impact structure, Ukraine, and its ejecta deposits. *Meteoritics & Planetary Science* **44**, 389–404.

HALLAM, A. 1993. Major bio-events in the Triassic and Jurassic. In *Global Events and Event Stratigraphy in the Phanerozoic* (ed. O. H. Walliser), pp. 265–283. Heidelberg: Springer.

HALLAM, A. 1995. Oxygen-restricted facies of the basal Jurassic of north west Europe. *Historical Biology* **10**, 247–57.

HALLAM, A. & WIGNALL, P. B. 1997. *Mass Extinctions and their Aftermath*. Oxford: Oxford University Press.

HALLAM, A., WIGNALL, P. B., YIN, J. & RIDING, J. B. 2000. An investigation into possible facies changes across the Triassic-Jurassic boundary in southern Tibet. *Sedimentary Geology* **137**, 101–6.

HARFOOT, M. B., PYLE, J. A. & BEERLING, D. J. 2008. End-Permian ozone shield unaffected by oceanic hydrogen sulphide and methane releases. *Nature Geoscience* **1**, 247–52.

HAUTMANN, M. 2004. Effect of end-Triassic CO_2 maximum on carbonate sedimentation and marine mass-extinction. *Facies* **50**, 257–61.

HAUTMANN, M., BENTON, M. J. & TOMASOVYCH, A. 2008. Catastrophic ocean acidification at the Triassic-Jurassic boundary. *Neues Jahrbuch für Geologie und Paläontologie, Abhandlungen* **249**, 119–27.

HAYS, L. E., BEATTY, T., HENDERSON, C. M., LOVE, G. D. & SUMMONS, R. E. 2007. Evidence for photic zone euxinia through the end-Permian mass extinction in the Panthalassic Ocean (Peace River Basin, Western Canada). *Palaeoworld* **16**, 39–50.

HERMANN, E., HOCHULI, P. A., BUCHER, H., BRÜHWILER, T., HAUTMANN, M., WARE, D. & ROOHI, G. 2011. Terrestrial ecosystems on North Gondwana following the end-Permian mass extinction. *Gondwana Research* **20**, 630–7.

HESSELBO, S. P., MCROBERTS, C. A. & PALFY, J. 2007. Triassic-Jurassic boundary events: Problems, progress, possibilities. *Palaeogeography, Palaeoclimatology, Palaeoecology* **244**, 1–10.

HESSELBO, S. P., ROBINSON, S. A., SURLYK, F. & PIASECKI, S. 2002. Terrestrial and marine extinction at the Triassic-Jurassic boundary synchronized with major carbon cycle perturbation: a link to initiation of massive volcanism. *Geology* **30**, 251–4.

HEUNISCH, C., LUPPOLD, F. W., REINHARDT, L. & RÖHLING, H.-G. 2010. Palynofazies, Bio-, und Lithostratigraphie im Grenzbereich Trias/Jura in der Bohrung Mariental I (Lappwaldmulde, Ostniedersachsen). *Zeitschrift der Deutschen Geologischen Gesellschaft* **161**, 51–98.

HOCHULI, P. A., VIGRAN, J. O., HERMANN, E. & BUCHER, H. 2010. Multiple climatic changes around the Permian-Triassic boundary event revealed by an expanded palynological record from mid-Norway. *Geological Society of America Bulletin* **122**, 884–96.

HOEGH-GULDBERG, O., MUMBY, P. J., HOOTEN, A. J., STENECK, R. S., GREENFIELD, P., GOMEZ, E., HARVELL, C. D., SALE, P. F., EDWARDS, A. J., CALDEIRA, K., KNOWLTON, N., EAKIN, C. M., IGLESIAS-PRIETO, R., MUTHIGA, N., BRADBURY, R. H., DUBI, A. &

HATZIOLOS, M. E. 2007. Coral reefs under rapid climate change and ocean acidification. *Science* **318**, 1737–42.

HOLSTEIN, B. 2004. Palynologische Untersuchungen der Kössener Schichten (Rhät, Alpine Obertrias). *Jahresbericht der Geologischen Bundesanstalt* **144**, 261–365.

HORI, R. S., FUJIKI, T., INOUE, E. & KIMURA, J.-I. 2007. Platinum group element anomalies and bio-events in the Triassic–Jurassic deep-sea sediments of Panthalassa. *Palaeogeography, Palaeoclimatology, Palaeoecology* **244**, 391–406.

HUDSPITH, V. A., RIMMER, S. M. & BELCHER, C. M. 2014. Latest Permian chars may derive from wildfires, not coal combustion. *Geology* **42**, 879–82.

HUYNH, T. T. & POULSEN, C. J. 2005. Rising atmospheric CO_2 as a possible trigger for the end-Triassic mass extinction. *Palaeogeography, Palaeoclimatology, Palaeoecology* **217**, 223–42.

IPCC, 2014. Climate Change 2014: Synthesis Report. Contribution of Working Groups I, II and III to the Fifth Assessment Report of the Intergovernmental Panel on Climate Change (eds Core Writing Team, R. K. Pachauri & L. A. Meyer). Geneva, Switzerland: IPCC, 151 pp.

ISOZAKI, Y. 1997. Permian-Triassic boundary super anoxia and stratified superocean: records from lost deep sea. *Science* **276**, 235–38.

JADOUL, F. & GALLI, M. T. 2008. The Hettangian shallow water carbonates after the Triassic-Jurassic biocalcification crisis: The Albenza Formation in the western Southern Alps. *Rivista Italiana di Paleontologia e Stratigrafia* **114**, 453–70.

JARAULA, C. M. B., GRICE, K., TWITCHETT, R. J., BÖTTCHER, M. E., LEMETAYER, P., DASTIDAR, A. G. & OPAZO, L. F. 2013. Elevated pCO_2 leading to Late Triassic extinction, persistent photic zone euxinia, and rising sea levels. *Geology* **41**, 955–8.

JOACHIMSKI, M. M., LAI, X., SHEN, S., JIANG, H., LUO, G., CHEN, B., CHEN, J. & SUN, Y. 2012. Climate warming in the latest Permian and the Permian-Triassic mass extinction. *Geology* **40**, 195–8.

KAMPSCHULTE, A. & STRAUSS, H. 2004. The sulfur isotopic evolution of Phanerozoic seawater based on the analysis of structurally substituted sulfate in carbonates. *Chemical Geology* **204**, 255–86.

KASPRAK, A. H., SEPULVEDA, J., PRICE-WALDMAN, R., WILLIFORD, K. H., SCHOEPFER, S. D., HAGGART, J. W., WARD, P. D., SUMMONS, R. E. & WHITESIDE, J. H. 2015. Episodic photic zone euxinia in the northeastern Panthalassic Ocean during the end-Triassic extinction. *Geology* **43**, 307–10.

KATZ, M. E., WRIGHT, J. D., MILLER, K. G., CRAMER, B. S., FENNEL, K. & FALKOWSKI, P. G. 2005. Biological overprint of the geological carbon cycle. *Marine Geology* **217**, 323–38.

KERSHAW, S., ZHANG, T. & LAN, G. 1999. A ?microbialite carbonate crust at the Permian-Triassic boundary in South China, and its palaeoenvironmental significance. *Palaeogeography, Palaeoclimatology, Palaeoecology* **146**, 1–18.

KIESSLING, W., ABERHAN, M., BRENNEIS, B. & WAGNER, P. J. 2007. Extinction trajectories of benthic organisms across the Triassic–Jurassic boundary. *Palaeogeography, Palaeoclimatology, Palaeoecology* **244**, 201–22.

KNIGHT, K. B., NOMADE, S., RENNE, P. R., MARZOLI, A., BERTRAND, H. & YOUBI, N. 2004. The Central Atlantic Magmatic Province at the Triassic-Jurassic boundary: paleomagnetic and $^{40}Ar/^{39}Ar$ evidence from Morocco for brief, episodic volcanism. *Earth and Planetary Science Letters* **228**, 143–60.

KNOLL, A. H., BAMBACH, R. K., CANFIELD, D. E. & GROTZINGER, J. P. 1996. Comparative Earth history and Late Permian mass extinction. *Science* **273**, 452–7.

KNOLL, A. H., BAMBACH, R. K., PAYNE, J. L., PRUSS, S. & FISCHER, W. W. 2007. Paleophysiology and end-Permian mass-extinction. *Earth and Planetary Science Letters* **256**, 295–313.

KORTE, C., HESSELBO, S. P., JENKYNS, H. C., RICKABY, R. E. M. & SPÖTL, C. 2009. Palaeoenvironmental significance of carbon and oxygen-isotope stratigraphy of marine Triassic-Jurassic boundary sections in SW Britain. *Journal of the Geological Society of London* **166**, 431–45.

KUMP, L. R., PAVLOV, A. & ARTHUR, M. A. 2005. Massive release of hydrogen sulfide to the surface ocean and atmosphere during intervals of oceanic anoxia. *Geology* **33**, 397–400.

KURODA, J., HORI, R. S., SUZUKI, K., GRÖCKE, D. R. & OHKOUCHI, N. 2010. Marine osmium isotope record across the Triassic-Jurassic boundary from a Pacific pelagic site. *Geology* **38**, 1095–8.

KÜRSCHNER, W. M., BATENBURG, S. J. & MANDER, L. 2013. Aberrant *Classopollis* pollen reveals evidence for unreduced (2n) pollen in the conifer family Cheirolepidiaceae during the Triassic-Jurassic transition. *Proceedings of the Royal Society of London, Series B* **280**, 20131708.

LEHRMANN, D. J., BENTZ, J. M., WOOD, T., GOERS, A., DHILLON, R., AKIN, S., LI, X., PAYNE, J. L., KELLEY, B. M., MEYER, K. M., SCHAAL, E. K., SUAREZ, M. B., YU, M., QIN, Y., LI, R., MINZONI, M. & HENDERSON, C. M. 2015. Environmental controls on the genesis of marine microbialites and dissolution surface associated with the end-Permian mass-extinction: New sections and observations from the Nanpanjiang Basin, South China. *Palaios* **30**, 529–52.

LINDSTRÖM, S., PEDERSEN, G. K., VAN DE SCHOOTBRUGGE, B., HANSEN, K. H., KUHLMANN, N., THEIN, J., JOHANSSON, L., PETERSEN, H. I., AWLMARK, C., DYBKJAER, K., WEIBEL, R., ERLSTROM, M., NIELSEN, L. H., OSCHMANN, W. & TEGNER, C. 2015. Intense and widespread seismicity during the end-Triassic mass-extinction due to emplacement of a large igneous province. *Geology* **43**, 387–90.

LINDSTRÖM, S., VAN DE SCHOOTBRUGGE, B., DYBKJAER, K., PEDERSEN, G. K., FIEBIG, J., NIELSEN, L. H. & RICHOZ, S. 2012. No causal link between terrestrial ecosystem change and methane release during the end-Triassic mass-extinction. *Geology* **40**, 531–4.

LOOY, C. V., TWITCHETT, R. J., DILCHER, D. L., VAN KONIJNENBURG-VAN CITTERT, J. H. A. & VISSCHER, H. 2001. Life in the end-Permian dead zone. *Proceedings of the National Academy of Science* **98**, 7879–83.

MANDER, L., TWITCHETT, R. J. & BENTON, M. J. 2008. Palaeoecology of the Late Triassic extinction event in the SW UK. *Journal of the Geological Society of London* **165**, 319–32.

MARTEL, A., BLOOI, M., ADRIAENSEN, C., VAN ROOIJ, P., BEUKEMA, W., FISHER, M. C., FARRER, R. A., SCHMIDT, B. R., TOBLER, U., GOKA, K., LIPS, K. R., MULETZ, C., ZAMUDIO, K. R., BOSCH, J., LOTTERS, S., WOMBWELL, E., GARNER, T. W. J., CUNNINGHAM, A. A., SPITZEN-VAN DER SLUIJS, A., SALVIDIO, S., DUCATELLE, R., NISHIKAWA, K., NGUYEN, T. T., KOLBY, J. E., VAN BOCXLAER, I., BOSSUYT, F. & PASMANS, F. 2014.

Recent introduction of a chytrid fungus endangers Western Palearctic salamanders. *Science* **346**, 630–1.

MARTINDALE, R. C., BERELSON, W. M., CORSETTI, F. A., BOTTJER, D. J. & WEST, A. J. 2012. Constraining carbonate chemistry at a potential ocean acidification event (the Triassic–Jurassic boundary) using the presence of corals and coral reefs in the fossil record. *Palaeogeography, Palaeoclimatology, Palaeoecology* **350–352**, 114–23.

MARUOKA, T., KOEBERL, C., HANCOX, P. J. & REIMOLD, W. U. 2003. Sulfur geochemistry across a terrestrial Permian-Triassic boundary section in the Karoo Basin, South Africa. *Earth and Planetary Science Letters* **206**, 101–17.

MARYNOWSKI, L. & SIMONEIT, B. R. T. 2009. Widespread Upper Triassic to Lower Jurassic wildfire records from Poland: Evidence from charcoal and pyrolytic polycyclic aromatic hydrocarbons. *Palaios* **24**, 785–98.

MARZOLI, A., BERTRAND, H., KNIGHT, K., CIRILLI, S., BURATTI, N., VERATI, C., NOMADE, S., RENNE, P. R., YOUBI, N., MARTINI, R., ALLENBACH, K., NEUWERTH, R., RAPAILLE, C., ZANINETTI, L. & BELLIENI, G. 2004. Synchrony of the Central Magmatic Province and the Triassic-Jurassic boundary and biotic crisis. *Geology* **32**, 973–6.

MARZOLI, A., JOURDAN, F., PUFFER, J. H., CUPPONE, T., TANNER, L. H., WEEMS, R. E., BERTRAND, H., CIRILLI, S., BELLIENI, G. & DE MIN, A. 2011. Timing and duration of the Central Atlantic Magmatic Province in the Newark and Culpeper Basins, eastern USA. *Lithos* **122**, 175–88.

MARZOLI, A., RENNE, P. R., PICCIRILLO, E. M., ERNESTO, A., BELLIENI, G. & DE MIN, A. 1999. Extensive 200-million-year-old continental flood basalts of the Central Atlantic Magmatic Province. *Science* **284**, 616–8.

MCELWAIN, J. C., BEERLING, D. J. & WOODWARD, F. I. 1999. Fossil plants and global warming at the Triassic-Jurassic boundary. *Science* **285**, 1386–90.

METCALFE, I., FOSTER, C. B., AFONIN, S. A., NICOLL, R. S., MUNDIL, R., XIAOFENG, W. & LUCAS, S. G. 2009. Stratigraphy, biostratigraphy and C-isotopes of the Permian–Triassic non-marine sequence at Dalongkou and Lucaogou, Xinjiang Province, China. *Journal of Asian Earth Sciences* **36**, 503–20.

MEYER, K. M. & KUMP, L.R. 2008. Oceanic euxinia in Earth history: causes and consequences. *Annual Review Earth and Planetary Sciences* **36**, 251–88.

MEYER, K. M., KUMP, L. R. & RIDGWELL, A. 2008. Biogeochemical controls on photic-zone euxinia during the end-Permian mass extinction. *Geology* **36**, 747–50.

MEYER, K. M., YU, M., JOST, A. B., KELLEY, B. M. & PAYNE, J. L. 2011. $\delta^{13}C$ evidence that high primary productivity delayed recovery from end-Permian mass extinction. *Earth and Planetary Science Letters* **302**, 378–84.

MURPHY, R. R., KEMP, W. M. & BALL, W. P. 2011. Long-term trends in Chesapeake Bay seasonal hypoxia, stratification, and nutrient loading. *Estuaries and Coasts* **34**, 1293–309.

NABBEFELD, B., GRICE, K., SUMMONS, R. E., HAYS, L. E. & CAO, C. 2010. Significance of polycyclic aromatic hydrocarbons (PAHs) in Permian/Triassic boundary sections. *Applied Geochemistry* **25**, 1374–82.

NEWELL, A. J., SENNIKOV, A. G., BENTON, M. J., MOLOSTOVSKAYA, I. I., GOLUBEV, V. K., MINIKH, A. V. & MINIKH, M. G. 2010. Disruption of playa-lacustrine depositional systems at the Permo-Triassic boundary: evidence from Vyazniki and Gorokhovets on the Russian Platform. *Journal of the Geological Society of London* **167**, 695–716.

NEWTON, R. J., PEVITT, E. L., WIGNALL, P. B. & BOTTRELL, S. H. 2004. Large shifts in the isotopic composition of seawater sulphate across the Permo–Triassic boundary in northern Italy. *Earth and Planetary Science Letters* **218**, 331–45.

NOMADE, S., KNIGHT, K. B., BEUTEL, E., RENNE, P. R., VERATI, C., FERAUD, G., MARZOLI, A., YOUBI, N. & BERTRAND, H. 2006. Chronology of the Central Atlantic Magmatic Province: Implications for the central Atlantic rifting processes and the Triassic-Jurassic biotic crisis. *Palaeogeography, Palaeoclimatology, Palaeoecology* **244**, 324–42.

OLSEN, P. E., KENT, D. V., SUES, H-D., KOEBERL, C., HUBER, H., MONTANARI, A., RAINFORTH, E. C., FOWELL, S. J., SZAJINA, M. J. & HARTLINE, B. 2002. Ascent of dinosaurs linked to an iridium anomaly at the Triassic-Jurassic boundary. *Science* **296**, 1305–7.

PALFY, J. 2003. Volcanism of the Central Atlantic Magmatic Province as a potential driving force in the end-Triassic mass-extinction. In *The Central Atlantic Magmatic Province: Insights from Fragments of Pangea* (eds W. Hames, J.G. Mchone, P. Renne & C. Ruppel), pp. 255–67. Washington, DC: American Geophysics Union.

PAYNE, J. L. & CLAPHAM, M. E. 2012. End-Permian mass extinction in the oceans: an ancient analog for the twenty-first century? *Annual Review of Earth and Planetary Sciences* **40**, 89–111.

PAYNE, J. L., LEHRMANN, D. J., FOLLETT, D., SEIBEL, M., KUMP, L. R., RICCARDI, A., ALTINER, D., SANO, H. & WEI, J. 2007. Erosional truncation of uppermost Permian shallow-marine carbonates and implications for Permian-Triassic boundary events. *Geological Society of America Bulletin* **119**, 771–84.

PAYNE, J. L., LEHRMANN, D. J., WEI, J. Y., ORCHARD, M. J., SCHRAG, D. P. & KNOLL, A. H. 2004. Large perturbations of the carbon cycle during recovery from the end-Permian extinction. *Science* **305**, 506–9.

PIENKOWSKI, G., NIEDZWIEDZKI, G. & BRANSKI, P. 2014. Climatic reversals related to the Central Atlantic Magmatic Province caused the end-Triassic biotic crisis - Evidence from continental strata in Poland. In *Volcanism, Impacts, and Mass-Extinctions: Causes and Effects* (eds G. Keller & A. Kerr). Boulder: Geological Society of America.

PIENKOWSKI, G., NIEDZWIEDZKI, G. & WAKSMUNDZKA, M. 2012. Sedimentological, palynological and geochemical studies of the terrestrial Triassic–Jurassic boundary in northwestern Poland. *Geological Magazine* **149**, 308–32.

REICHOW, M. K., PRINGLE, M. S., AL'MUKHAMEDOV, A. I., ALLEN, M. B., ANDREICHEV, V. L., BUSLOV, M. M., DAVIES, C. E., FEDOSEEV, G. S., FITTON, J. G., INGER, S., MEDVEDEV, A. Y., MITCHELL, C., PUCHKOV, V. N., SAFONOVA, I. Y., SCOTT, R. A. & SAUNDERS, A. D. 2009. The timing and extent of the eruption of the Siberian Traps large igneous province: Implications for the end-Permian environmental crisis. *Earth and Planetary Science Letters* **277**, 9–20.

REINEMUND, J. A. 1955. *Geology of the Deep River coal field North Carolina*. Geological Survey Professional Paper 246, pp. 159.

RETALLACK, G. J. 2013. Permian and Triassic greenhouse crises. *Gondwana Research* **24**, 90–103.

RICCARDI, A. L., ARTHUR, M. A. & KUMP, L. R. 2006. Sulfur isotopic evidence for chemocline upward excursions during the end-Permian mass extinction. *Geochimica et Cosmochimica Acta* **70**, 5740–52.

RICHOZ, S., van DE SCHOOTBRUGGE, B., PROSS, J., PÜTTMANN, W., QUAN, T. M., LINDSTRÖM, S., HEUNISCH, C., FIEBIG, J., MAQUIL, R., HAUZENBERGER, C., SCHOUTEN, S. & WIGNALL, P. B. 2012. Hydrogen sulphide poisoning of shallow seas due to end-Triassic global warming. *Nature Geoscience* **5**, 662–7.

ROHR, J. R., RAFFEL, T. R., ROMANSIC, J. M., MCCALLUM, H. & HUDSON, P. J. 2008. Evaluating the links between climate, disease spread, and amphibian declines. *Proceedings of the National Academy of Science* **105**, 17436–41.

ROMANO, R., MASETTI, D., BARATTOLO, F., CARRAS, N., BARATTOLO, F. & ROGHI, G. 2008. The Triassic/Jurassic boundary in a peritidal carbonate platform of the Pelagonian Domain: The Mount Messapion section (Chalkida, Greec). *Rivista Italiana di Paleontologia e Stratigrafia* **114**, 431–52.

ROOPNARINE, P. D. 2006. Extinction cascades and catastrophe in ancient food webs. *Paleobiology* **32**, 1–19.

RUHL, M., BONIS, N. R., REICHART, G.-J., SINNINGHE DAMSTE, J. S. & KÜRSCHNER, W. 2011. Atmospheric carbon injection linked to end-Triassic mass-extinction. *Science* **333**, 430–4.

RUHL, M., DEENEN, M. H. L., ABELS, H. A., BONIS, N. R., KRIJGSMAN, W. & KÜRSCHNER, W. 2010. Astronomical constraints on the duration of the Early Jurassic Hettangian stage and recovery rates following the end-Triassic mass-extinction (St Audrie's Bay/East Quantoxhead, UK). *Earth and Planetary Science Letters* **295**, 262–76.

SCHALLER, M. F., WRIGHT, J. D. & KENT, D. V. 2011. Atmospheric pCO_2 perturbations associated with the Central Atlantic Magmatic Province. *Science* **331**, 1404–9.

SCHALLER, M. F., WRIGHT, J. D., KENT, D. V. & OLSEN, P. E. 2012. Rapid emplacement of the Central Atlantic Magmatic Province as a net sink for CO_2. *Earth and Planetary Science Letters* **323–324**, 27–39.

SCHALTEGGER, U., GUEX, J., BARTOLINI, A., SCHOENE, B. & OVTCHAROVA, M. 2008. Precise U-Pb age constraints for end-Triassic mass extinction, its correlation to volcanism and Hettangian post-extinction recovery. *Earth and Planetary Science Letters* **267**, 266–75.

SCHMIEDER, M., BUCHNER, E., SCHWARZ, W. H., TRIELOFF, M. & LAMBERT, P. 2010. A Rhaetian $^{40}Ar/^{39}Ar$ age for the Rochechouart impact structure (France) and implications for the latest Triassic sedimentary record. *Meteoritics & Planetary Science* **45**, 1225–42.

SCHMIEDER, M., JOURDAN, F., TOHVER, E. & CLOUTIS, E. A. 2014. $^{40}Ar/^{39}Ar$ age of the Lake Saint Martin impact structure (Canada): Unchaining the Late Triassic terrestrial impact craters. *Earth and Planetary Science Letters* **406**, 37–48.

SCHOBBEN, M., JOACHIMSKI, M. M., KORN, D., LEDA, L. & KORTE, C. 2014. Palaeotethys seawater temperature rise and an intensified hydrological cycle following the end-Permian mass extinction. *Gondwana Research* **26**, 675–83.

SCHOENE, B., GUEX, J., BARTOLINI, A., SCHALTEGGER, U. & BLACKBURN, T. J. 2010. Correlating the end-Triassic mass extinction and flood basalt volcanism at the 100 ka level. *Geology* **38**, 387–90.

SELF, S., WIDDOWSON, M., THORDARSON, T. & JAY, A. E. 2006. Volatile fluxes during flood basalt eruptions and potential effects on the global environment: A Deccan perspective. *Earth and Planetary Science Letters* **248**, 518–32.

SEPHTON, M. A., JIAO, D., ENGEL, M. H., LOOY, C. V. & VISSCHER, H. 2015. Terrestrial acidification during the end-Permian biosphere crisis. *Geology* **43**, 159–63.

SEPHTON, M. A., LOOY, C. V., BRINKHUIS, H., WIGNALL, P. B., DE LEEUW, J. W. & VISSCHER, H. 2005. Catastrophic soil erosion during the end-Permian biotic crisis. *Geology* **33**, 941–4.

SEPHTON, M. A., LOOY, C. V., VEEFKIND, R. J., VISSCHER, H., BRINKHUIS, H. & DE LEEUW, J. W. 1999. Cyclic diaryl ethers in a Late Permian sediment. *Organic Geochemistry* **30**, 267–73.

SEPKOSKI JR, J. J. 1987. Environmental trends in extinction during the Paleozoic. *Science* **235**, 64–6.

SEPKOSKI JR, J. J. 1996. Patterns of Phanerozoic extinction: a perspective from global data bases. In *Global Events and Event Stratigraphy in the Phanerozoic* (ed. O. H. Walliser), pp. 35–51. Berlin: Springer.

SHEN, S.-Z. & BOWRING, S. A. 2014. The end-Permian mass extinction: a still unexplained catastrophe. *National Science Review* **1**, 492–5.

SHEN, S.-Z., CAO, C.-Q., ZHANG, H., BOWRING, S. A., HENDERSON, C. M., PAYNE, J. L., DAVYDOV, V. I., CHEN, B., YUAN, D.-X., ZHANG, Y.-C., WANG, W. & ZHENG, Q.-F. 2013. High-resolution $\delta^{13}C_{carb}$ chemostratigraphy from latest Guadalupian through earliest Triassic in South China and Iran. *Earth and Planetary Science Letters* **375**, 156–65.

SHEN, S.-Z., CROWLEY, J. L., WANG, Y., BOWRING, S. A., ERWIN, D. H., SADLER, P. M., CAO, C. Q., ROTHMAN, D. H., HENDERSON, C. M., RAMEZANI, J., ZHANG, H., SHEN, Y., WANG, X. D., WANG, W., MU, L., LI, W. Z., TANG, Y. G., LIU, X. L., LIU, L. J., ZENG, Y., JIANG, Y. F. & JIN, Y. G. 2011*a*. Calibrating the end-Permian mass extinction. *Science* **334**, 1367–72.

SHEN, W., LIN, Y., XU, L., LI, J., WU, Y. & SUN, Y. 2007. Pyrite framboids in the Permian–Triassic boundary section at Meishan, China: Evidence for dysoxic deposition. *Palaeogeography, Palaeoclimatology, Palaeoecology* **253**, 323–31.

SHEN, W., SUN, Y., LIN, Y., LIU, D. & CHAI, P. 2011*b*. Evidence for wildfire in the Meishan section and implications for Permian–Triassic events. *Geochimica et Cosmochimica Acta* **75**, 1992–2006.

SIDDLE, H. V., KREISS, A., ELDRIDGE, M. D. B., NOONAN, E., CLARKE, C. J., PYECROFT, S., WOODS, G. M. & BELOV, K. 2007. Transmission of a fatal clonal tumor by biting occurs due to depleted MHC diversity in a threatened carnivorous marsupial. *Proceedings of the National Academy of Sciences* **104**, 16221–6.

SIMMS, M. J. 2003. Uniquely extensive seismite from the latest Triassic of the United Kingdom: evidence for bolide impact? *Geology* **31**, 557–60.

SMITH, R. M. H. & BOTHA-BRINK, J. 2014. Anatomy of a mass extinction: sedimentological and taphonomic evidence for drought-induced die-offs at the Permo-Triassic boundary in the main Karoo Basin, South Africa. *Palaeogeography, Palaeoclimatology, Palaeoecology* **396**, 99–118.

SOBOLEV, S. V., SOBOLEV, A. V., KUZMIN, D. V., KRIVOLUTSKAYA, N. A., PETRUNIN, A. G., ARNDT, N. T., RADKO, V. A. & VASILIEV, Y. R. 2011. Linking mantle plumes, large igneous provinces and environmental catastrophes. *Nature* **477**, 312–6.

SONG, H. J., WIGNALL, P. B., CHU, D., TONG, J., SUN, Y., SONG, H., HE, W. & TIAN, L. 2014. Anoxia/high temperature double whammy during the Permian-Triassic marine crisis and its aftermath. *Scientific Reports* **4**, 4132.

SONG, H. J., WIGNALL, P. B., TONG, J. & YIN, H. 2013. Two pulses of extinction during the Permian-Triassic crisis. *Nature Geoscience* **6**, 52–6.

SPRAY, J. G., KELLEY, S. P. & ROWLEY, D. B. 1998. Evidence for a late Triassic multiple impact event on Earth. *Nature* **392**, 171–3.

STANLEY JR, G. D. 1988. The history of early Mesozoic reef communities: a three step process. *Palaios* **3**, 170–83.

STANLEY JR, G. D. 2003. The evolution of modern corals and their early history. *Earth-Science Reviews* **60**, 195–225.

STANLEY JR, G. D. & BEAUVAIS, L. 1994. Corals from an Early Jurassic coral reef in British Columbia: refuge on an oceanic island reef. *Lethaia* **27**, 35–47.

STEINER, M. B., ESHET, Y., RAMPINO, M. R. & SCHWINDT, D. M. 2003. Fungal abundance spike and the Permian-Triassic boundary in the Karoo Supergroup (South Africa). *Palaeogeography, Palaeoclimatology, Palaeoecology* **194**, 405–14.

STEINTHORSDOTTIR, M., JERAM, A. J. & MCELWAIN, J. C. 2011. Extremely elevated CO_2 concentrations at the Triassic/Jurassic boundary. *Palaeogeography, Palaeoclimatology, Palaeoecology* **308**, 418–32.

STEVENS, R. B. 1960. Cultural practices in disease control. In *Plant Pathology and Advanced Treatise* (eds J. G. Horsfall & A. E. Dimonds), pp. 357–429. New York: Academic Press.

SUN, Y., JOACHIMSKI, M. M., WIGNALL, P. B., YAN, C., CHEN, Y., JIANG, H., WANG, L. & LAI, X. 2012. Lethally hot temperatures during the Early Triassic greenhouse. *Science* **338**, 366–70.

SVENSEN, H., PLANKE, S., POLOZOV, A. G., SCHMIDBAUER, N., CORFU, F., PODLADCHIKOV, Y. Y. & JAMTVEIT, B. 2009. Siberian gas venting and the end-Permian environmental crisis. *Earth and Planetary Science Letters* **277**, 490–500.

TANNER, L. H., KYTE, F. T. & WALKER, A. E. 2008. Multiple Ir anomalies in uppermost Triassic to Jurassic-age strata of the Blomidon Formation, Fundy basin, eastern Canada. *Earth and Planetary Science Letters* **274**, 103–11.

TANNER, L. H., LUCAS, S. G. & CHAPMAN, M. G. 2004. Assessing the record and causes of Late Triassic extinctions. *Earth-Science Reviews* **65**, 103–39.

TANNER, L. H., SMITH, D. L. & ALLAN, A. 2007. Stomatal response of swordfern to volcanogenic CO_2 and SO_2 from Kilauea volcano. *Geophysical Research Letters* **34**, 1–5 L15807.

TOMLINSON, G. H. 2003. Acid deposition, nutrient leaching and forest growth. *Biogeochemistry* **65**, 51–81.

TWITCHETT, R. J. 1999. Palaeoenvironments and faunal recovery after the end-Permian mass extinction. *Palaeogeography, Palaeoclimatology, Palaeoecology* **154**, 27–37.

TWITCHETT, R. J., KRYSTYN, L., BAUD, A., WHEELEY, J. R. & RICHOZ, S. 2004. Rapid marine recovery after the end-Permian mass-extinction event in the absence of marine anoxia. *Geology* **32**, 805–8.

UHL, D. & MONTENARI, M. 2011. Charcoal as evidence of palaeo-wildfires in the Late Triassic of SW Germany. *Geological Journal* **46**, 34–41.

ULRICH, B. 1990. Waldsterben: forest decline in West Germany. *Environmental Science and Technology* **24**, 436.

VAN DE SCHOOTBRUGGE, B., BACHAN, A., SUAN, G., RICHOZ, S. & PAYNE, J. L. 2013. Microbes, mud, and methane: Cause and consequence of recurrent Early Jurassic anoxia following the end-Triassic mass-extinction. *Palaeontology* **56**, 685–709.

VAN DE SCHOOTBRUGGE, B., PAYNE, J. L., TOMASOVYCH, A., PROSS, J., FIEBIG, J., BENBRAHIM, M., FÖLLMI, K. B. & QUAN, T. M. 2008. Carbon cycle perturbation and stabilization in the wake of the Triassic-Jurassic boundary mass-extinction event. *Geochemistry, Geophysics, Geosystems* **9**, Q04028.

VAN DE SCHOOTBRUGGE, B., QUAN, T., LINDSTRÖM, S., PÜTTMANN, W., HEUNISCH, C., PROSS, J., FIEBIG, J., PETSCHICK, R., RÖHLING, H.-G., RICHOZ, S., ROSENTHAL, Y. & FALKOWSKI, P. G. 2009. Floral changes across the Triassic-Jurassic boundary linked to flood basalt volcanism. *Nature Geoscience* **2**, 489–594.

VAN DE SCHOOTBRUGGE, B., TREMOLADA, F., BAILEY, T. R., ROSENTHAL, Y., FEIST-BURKHARDT, S., BRINKHUIS, H., PROSS, J., KENT, D. V. & FALKOWSKI, P. G. 2007. End-Triassic calcification crisis and blooms of organic-walled disaster species. *Palaeogeography, Palaeoclimatology, Palaeoecology* **244**, 126–41.

VISSCHER, H., BRINKHUIS, H., DILCHER, D. L., ELSIK, W. C., ESHET, Y., LOOY, C. V., RAMPINO, M. R. & TRAVERSE, A. 1996. The terminal Paleozoic fungal event: evidence of terrestrial ecosystem destabilisation. *Proceedings of the National Academy of Sciences* **93**, 2155–8.

VISSCHER, H., LOOY, C. V., COLLINSON, M. E., BRINKHUIS, H., VAN KONIJNENBURG-CITTERT, J. H. A., KÜRSCHNER, W. M. & SEPHTON, M. A. 2004. Environmental mutagenesis during the end-Permian ecological crisis. *Proceedings of the National Academy of Sciences* **101**, 12952–6.

VISSCHER, H., SEPHTON, M. A. & LOOY, C. V. 2011. Fungal virulence at the time of the end-Permian biosphere crisis? *Geology* **39**, 883–6.

WAKE, D. B. & VREDENBURG, V. T. 2008. Are we in the midst of the sixth mass extinction? A view from the world of amphibians. *Proceedings of the National Academy of Science* **105**, 11466–73.

WANG, Y., SADLER, P. M., SHEN, S-Z., ERWIN, D. H., ZHANG, Y.-C., WANG, X.-D., WANG, W., CROWLEY, J. L. & HENDERSON, C. M. 2014. Quantifying the process and abruptness of the end-Permian mass-extinction. *Palaeobiology* **40**, 113–29.

WARD, P. D., MONTGOMERY, D. R. & SMITH, R. 2000. Altered river morphology in South Africa related to the Permian-Triassic extinction. *Science* **289**, 1740–3.

WARGO, P. M. 1996. Consequences of environmental stress on oak: predisposition to pathogens. *Annals of Science Forum* **53**, 359–68.

WATSON, J. S., SEPHTON, M. A., LOOY, C. V. & GILMOUR, I. 2005. Oxygen-containing aromatic compounds in a Late Permian sediment. *Organic Geochemistry* **36**, 371–84.

WHITESIDE, J. H., OLSEN, P. E., EGLINTON, T., BROOKFIELD, M. E. & SAMBROTTO, R. N. 2010. Compound-specific carbon isotopes from Earth's largest flood basalt eruptions directly linked to the end-Triassic mass-extinction. *Proceedings of the National Academy of Sciences* **107**, 6721–5.

WIGNALL, P. B. 2001*a*. Large igneous provinces and mass extinctions. *Earth-Science Reviews* **53**, 1–33.

WIGNALL, P. B. 2001*b*. Sedimentology of the Triassic-Jurassic boundary beds in Pinhay Bay (Devon, SW England). *Proceedings of the Geologists' Association* **112**, 349–60.

WIGNALL, P. B. 2015. *The Worst of Times: 80 million years of Extinction: How Life on Earth Survived Eighty Million Years of Extinctions.* Princeton: Princeton University Press.

WIGNALL, P. B. & BOND, D. P. G. 2008. The end-Triassic and Early Jurassic mass extinction records in the British Isles. *Proceedings of the Geologists' Association* **119**, 73–84.

WIGNALL, P. B., BOND, D. P. G., KUWAHARA, K., KAKUWA, Y., NEWTON, R. J. & POULTON, S. W. 2010. An 80 million year oceanic redox history from the Permian to Jurassic pelagic sediments of the Mino-Tamba terrane, SW Japan, and the origin of four mass extinctions. *Global and Planetary Change* **71**, 109–23.

WIGNALL, P. B. & HALLAM, A. 1992. Anoxia as a cause of the Permian/Triassic mass extinction: facies evidence from northern Italy and the western United States. *Palaeogeography, Palaeoclimatology, Palaeoecology* **93**, 21–46.

WIGNALL, P. B., NEWTON, R. & BROOKFIELD, M. E. 2005. Pyrite framboid evidence for oxygen-poor deposition during the Permian-Triassic crisis in Kashmir. *Palaeogeography, Palaeoclimatology, Palaeoecology* **216**, 183–8.

WIGNALL, P. B. & TWITCHETT, R. J. 2002. Extent, duration, and nature of the Permian-Triassic superanoxic event. In *Catastrophic Events and Mass Extinctions; Impacts and Beyond* (ed. K. G. MacLeod), pp. 395–413. Boulder, Colorado: Geological Society of America.

WIGNALL, P. B., ZONNEVELD, J.-P., NEWTON, R. J., AMOR, K., SEPHTON, M. A. & HARTLEY, S. 2007. The end Triassic mass-extinction record of Williston Lake, British Columbia. *Palaeogeography, Palaeoclimatology, Palaeoecology* **253**, 385–406.

WILLIFORD, K. H., FORIEL, J., WARD, P. D. & STEIG, E. J. 2009. Major perturbation in sulfur cycling at the Triassic-Jurassic boundary. *Geology* **37**, 835–8.

WILLIFORD, K. H., GRICE, K., HOLMAN, A. & MCELWAIN, J. C. 2014. An organic record of terrestrial ecosystem collapse and recovery at the Triassic–Jurassic boundary in East Greenland. *Geochimica et Cosmochimica Acta* **127**, 251–63.

WINNER, W. E. & MOONEY, H. A. 1980*a*. Ecology of SO_2 resistance: II. Photosynthetic changes of shrubs in relation to SO_2 absorption and stomatal behavior. *Oecologia* **44**, 296–302.

WINNER, W. E. & MOONEY, H.A. 1980*b*. Ecology of SO_2 resistance: III. Metabolic changes of C3 and C4 Atriplex species due to SO_2 fumigation. *Oecologia* **46**, 49–54.

WOODS, A. D., BOTTJER, D. J., MUTTI, M. & MORRISON, J. 1999. Lower Triassic large sea-floor carbonate cements: their origin and a mechanism for the prolonged biotic recovery from the end-Permian mass extinction. *Geology* **27**, 645–8.

WOTZLAW, J.-F., GUEX, J., BARTOLINI, A., GALLET, Y., KRYSTYN, L., MCROBERTS, C. A., TAYLOR, D., SCHOENE, B. & SCHALTEGGER, U. 2014. Towards accurate numerical calibration of the Late Triassic: High-precision U-Pb geochronology constraints on the duration of the Rhaetian. *Geology* **42**, 571–4.

YÁÑEZ-LÓPEZ, R. 2012. The effect of climate change on plant diseases. *African Journal of Biotechnology* **11**, 2417–28.

ZAJZON, N., KRISTALY, F., PALFY, J. & NEMETH, T. 2012. Detailed clay mineralogy of the Triassic-Jurassic boundary section at Kendlbachgraben (Northern Calcareous Alps, Austria). *Clay Minerals* **47**, 177–89.